



ISSN 1349-1113
JAXA-RR-05-034E

JAXA Research and Development Report

Thermo-physical and atomic transport properties of liquid metals related to the experiments under microgravity

March 2006

Japan Aerospace Exploration Agency

目 次

序 文	正木匡彦
シアーセル法による溶融 Ag 中の Au の拡散係数測定	深澤智晴・正木匡彦・伊丹俊夫・渡邊勇基 ... 1
Current status of the development of shear cell technique in ground base research and towards JEM on ISS	T. Masaki, T. Fukazawa, S. Matsumoto, T. Itami and S. Yoda ... 8
Measurement of diffusion coefficient of Au in liquid Ag due to the shear cell technique	T. Masaki, T. Fukazawa, Y. Watanabe, M. Kaneko, S. Yoda and T. Itami ... 19
静電浮遊法による高温金属液体の構造解析	正木匡彦・石川毅彦・依田真一 ... 25

序 文

1970年代における微小重力科学実験の創世記より、材料熱物性値の高精度取得実験は、その主要なテーマのひとつとして多大な努力が注がれてきており、高温融体の拡散係数の高精度計測など大きな成果を挙げてきている。国際宇宙ステーションが稼動しつつある現在においても、スペースシャトル、回収カプセルや小型ロケットを用いた物性計測実験が国内外を問わず進められてきており、物性計測研究が依然として微小重力環境を利用した科学・技術研究の主要なターゲットのひとつであることに変わりはない。

本研究は、旧宇宙開発事業団宇宙環境利用研究システムの課題研究として進められてきた「拡散現象のモデル化研究」を発展させたものであり、高精度拡散係数測定技術や液体構造に基づく原子ダイナミクス of 理論研究手法を継承し、さらに将来の微小重力実験の実施へ向けた技術開発や理論の精緻化を進めているものである。本年は、この拡散現象の研究をさらに発展させ、また将来の宇宙実験の実施へ向けた開かれた研究コミュニティを形成するために、研究班ワーキンググループ「拡散問題研究会」を発足させ、測定技術などに関する情報交換や今後の方向性に関する議論を始めたところである。本論文は、その研究会における議論のたたき台のひとつとして、われわれの最新の研究成果をまとめたものである。本研究を礎のひとつとして、微小重力環境を利用した物性研究が大きく発展することを期待する。

宇宙環境利用科学研究系
正木 匡彦

シアーセル法による溶融 Ag 中の Au の拡散係数測定

深澤 智晴^{*1*2}, 正木 匡彦^{*2}, 伊丹 俊夫^{*2*3}, 渡邊 勇基^{*4}

Diffusion Coefficient Measurement of Au in Liquid Ag by Shear-Cell Method

By

Tomoharu Fukazawa^{*1*2}, Tadahiko Masaki^{*2}, Toshio Itami^{*2*3}, Yuki Watanabe^{*4}

Abstract: Shear cell method is one of the advanced experimental techniques to measure diffusion coefficients in liquids. In order to measure diffusion coefficient more accurately, we studied error factors of this method. The shear convection due to the shear cell method is one of the major error factors of the measurement of diffusion coefficient. To clarify effects of shear convection, we carried out the diffusion coefficient measurement of Au in liquid Ag at the temperatures of 1300 K and 1500 K with the variation of diffusion time. We obtained the diffusion time dependence of Au diffusion coefficient in liquid Ag. The errors due to the shear convection can be eliminated by adopting the diffusion time over 3 hours.

Keywords: shear cell, diffusion coefficient, liquid metals

概 要

シアーセル法は、融液の拡散係数を測定するためのもっとも優れた方法の一つである。我々は、シアーセル法を用いてより高精度な融液の拡散係数を獲得するため、本方法に潜在する誤差要因の特定とその対策を検討した。特に拡散係数の測定値に対する拡散対接合時の対流（シアー対流）の影響を明らかにするため、実験温度 1300 K および 1500 K において拡散時間をパラメータにとりモデル試料として AuAg 合金を採用して拡散実験を行った。溶融 Ag 中の Au の拡散係数の拡散保持時間依存性から拡散保持時間を 3 時間以上とすることでシアー対流の影響を排除することが可能であることが判明した。

1. 序 論

これまでの地上重力下において実施された高温融体中の拡散係数の測定は、重力による対流の悪影響を受けている。宇宙航空研究開発機構（以下 JAXA）では、現在、高温の金属や半導体融液を対象としたプロジェクト研究「拡散現象のモデル化及び高精度拡散係数測定研究」を進めており、無対流の宇宙微小重力環境下においてシアーセル法を用いた高温融体の高精度拡散係数測定を実施することを究極の目的としている。

シアーセル法は、従来行われてきたロングキャピラリー法を発展させ、液体状態において拡散試料の接合・分断を可能

-
- * 1 Ishikawajima Jet Service Co., Ltd., Space Utilization and Operations Gr., Space Department
Akishima Showa Bldg., 2(3F), 568-1, Tanakacho, akishima-city, Tokyo 196-0014 Japan
 - * 2 Japan Aerospace Exploration Agency, Institute of Space and Astronautical Science, ISS project office
2-1-1 Sengen, Tsukuba-city, Ibaraki, 305-8505 Japan
 - * 3 Graduate School of Science, Hokkaido University
Kita 10 Nishi 5, Sapporo 060-0810, Japan
 - * 4 Advanced Engineering Service Co., Ltd., Space Development Division
1-6-1 Takezono, Tsukuba-city, Ibaraki, 305-0032 Japan

とした方法である。これにより、この方法は昇温および冷却中の拡散、凝固時の偏析等による濃度分布の乱れなどの影響を排除することを可能とした高精度拡散係数測定法である。これまで、我々は地上実験用のシアーセルを製作し、モデル試料のAgAu合金を対象に、重力環境下での参照データの蓄積、および、シアーセル法の誤差要因の解明と高精度化を目的として研究を進めてきた。本報告では、まずシアーセル法による拡散係数測定技術の高精度化のために実施してきた改良点について述べる。

次にシアーセル法に固有の誤差要因であるシアー対流の影響と溶融Ag中のAuの拡散係数の拡散保持時間の関係についての検討結果について報告する。

2. シアーセル法

シアーセル法は、ロングキャピラリー法の欠点であった昇温・冷却過程での拡散の進行や、試料の溶融・凝固にともなう体積変化及び凝固時の偏析などに起因する濃度分布の測定誤差を排除した測定が可能な、融液の拡散係数測定方法の一つである。図1にその概念図を示す。シアーセル法では、拡散対は最初に離して配置した状態のまま加熱・溶融(①)し、所定の実験温度に到達後に接合(②)させる。そして、接合させた拡散対は所定の時間だけ拡散を進行(③)させた後、拡散時間の終了と共に細かく切断(④)させてから冷却・凝固(⑤)させる。このようなプロセスを経ることにより、本方法では先に述べた誤差要因の完全な排除を可能としている。

このシアーセル法に使用するつぼは、試料の接合・切断を行うため、複数の部品から構成されている。図2にシアーセルのつぼの概略図を示す。特に主要な部品として、中心穴と外周に、試料を接合・切断するときに回転角度を決定するための切欠きを持った厚さ1mmのディスクと、それらを束ねて回転させる回転軸、そして各々のディスクの回転角度を制御する固定キーなどがある。ディスクには直径1mmの試料穴が同心円上に2つないし3つ開いている。つぼの組立は、実験条件に応じた複数枚のディスクを、試料穴位置がそろるように積層し、それにより形成されたロングキャピラリー法のような細管に、棒状の拡散試料対を離した状態で挿入して完成する。実験中に回転軸を回転することにより、液体状態となった試料を容易に接合・切断できる機構となっている。

シアーセル法は、このような特殊な機構を持ったつぼを使用することにより、ロングキャピラリー法において誤差要

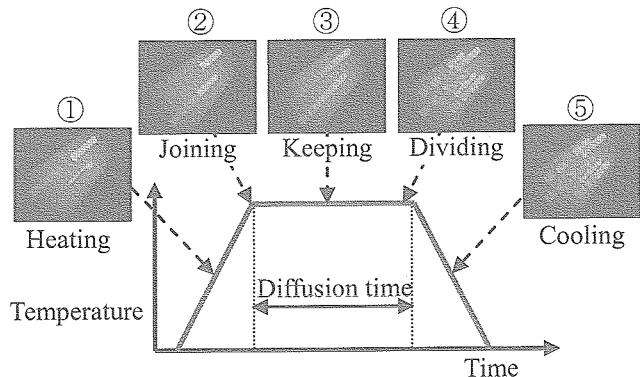


Fig. 1 Shear cell method.

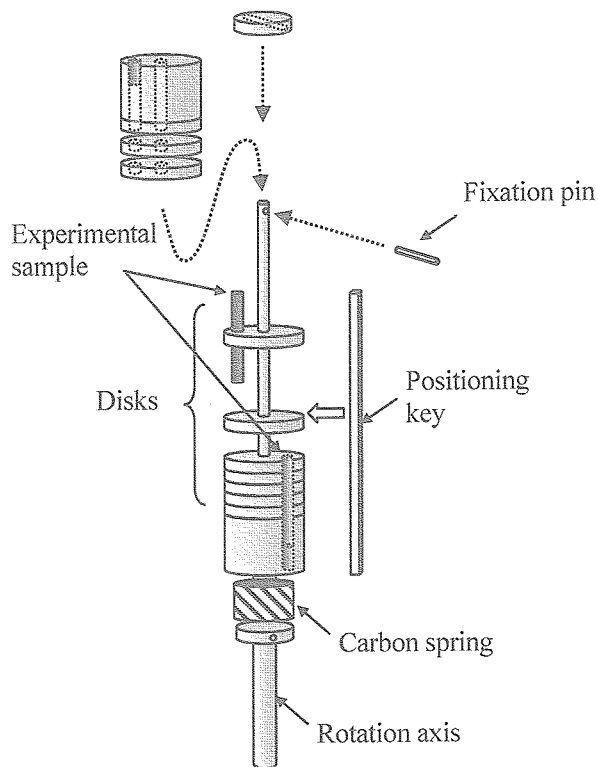


Fig. 2 Schematic figure of shear cell.

因となっていた欠点を除去した方法である。しかし、この方法にも、その構造・機構に由来する固有の誤差要因となる問題が存在する。それは、接合時の試料アライメント、および、シアー対流の問題である。そこで、特にシアー対流の問題に対して拡散保持時間をパラメータに実験を実施した。

2.1 接合時のズレ

シアーセル法では、始めに拡散対が離された状態で配置されるため、その接合が確実に行われなくては拡散の進行に問題が発生し拡散係数の測定値に影響を与える。しかし、実験中に試料の接合状態を確認することは、試料がるつぼの中に入れられた状態であるため困難である。そこで、るつぼ内の試料が正常に接合・切断されたことを確認するため、我々は試料の X 線による観察が可能なシアーセル実験装置（シアーセルカートリッジ）を開発した。図 3 にシアーセルカートリッジの外観を示す。本装置は、実験試料にあたる部分のるつぼ材にグラファイト、ヒーター材に焦性グラファイト/焦性ポロンナイトライド (PG/PBN) 製セラミックスヒーター、カートリッジ材に溶融アルミナ管と、X 線に対して透明な材料を選定し使用することにより試料のその場観察を可能としたものである。

X 線による観察は国際宇宙ステーション搭載予定の帯域炉 (AFEX) 地上炉に装備されている X 線観察装置 (図 3 右) を用いて行い、実験中の試料が接合・切断する様子を明瞭に確認することに成功した。

図 4 にシアーセルカートリッジを用いて AFEX により観察したシアーセル実験の X 線透過像の一例を示す。その結果、従来のるつぼ材料であるグラファイト材では試料の接合時に約 0.1 mm 程度のズレが生じていることが初めて明らかとなった。このズレはグラファイトの加工精度の向上により回避しなくてはならない。しかし、本材料は焼結品であるためこれ以上の加工精度の向上は困難であった。そこで、我々は、新たなるつぼ材料として機械的強度が優れ加工精度の高いグラスカーボン材料を選定し、新るつぼの製作を行った。本材料は公差 ± 0.02 mm 以下の精度での加工が可能であり、これを用いて製作したシアーセルによる実験ではズレの無い接合が可能となった (図 4)。

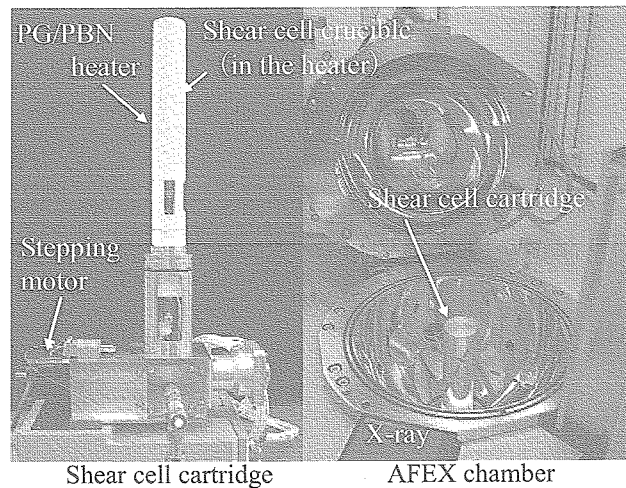


Fig. 3 Outlook of shear cell cartridge.

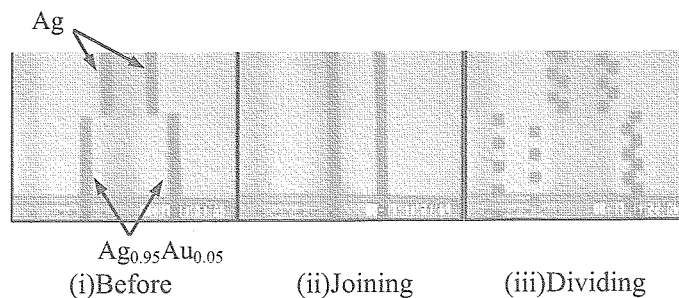


Fig. 4 In situ X-ray image of diffusion experiment (glassy carbon, Ag-Ag_{0.95}Au_{0.05}, 1300 K).

2.2 セルの面粗さおよび接合速度とシアー対流

シアーセル法では液体状態の試料を接合させるため、液体試料の接合面にせん断力による流れ（シアー対流）による擾乱が発生する。この現象はシアーセルに固有のものであり拡散係数の測定誤差の一因となる。図5に実験初期における試料の濃度分布の模式図を示す。

拡散時間 $t=0$ における拡散対界面の濃度分布は本来矩形でなくてはならない（図5左）。しかし、試料接合時のシアー対流により距離 Δx にわたり試料が混合し濃度分布に勾配が生じてしまう（図5右）。したがって、この状態の存在はすでに時間 Δt だけ拡散が進んだ状態から実験が開始されたものとして考慮することが出来る。この効果を含んだ結果として得られる拡散係数は、真の値に対してシアー対流の影響による見かけの拡散分だけ大きなものとなることが予想される。そこで、このシアー対流による擾乱を出来る限り抑制するため、シアーセルディスクの表面粗さ及び拡散対を接合する時の速度について、液体 Ag 中の Au の拡散実験により最適な実験条件の検討を行った。拡散実験の詳細は文献[2]を参照された。

図6に接合面のディスクの面粗さと拡散係数の測定値の関係を、また図7に拡散対の接合速度と拡散係数の測定値の関係を示す。これらの図で実験点に付けられた範囲はデータのばらつきを示している。したがって、範囲の付けられていない場合はばらつきが小さく実験点の大きさにばらつきの範囲が隠れている事を意味している。これらの結果から、試料組成、実験温度、および拡散時間が同一の条件では、接合面のセルの面粗さが粗く拡散対の接合速度が遅い方が、得られる拡散係数は、値が小さくばらつきも少ないことが明らかとなった。特に、接合速度の影響の結果はシアー時の対流の可視化による流体シミュレーション[3]と定性的に一致した。

2.3 シアー対流と拡散保持時間

前項にて議論したシアー対流は、実験条件の最適化によりその影響を抑制することが可能であることが明らかとなった。しかし、それを完全に排除することは困難である。そこで、我々はシアー対流が実験の初期にのみ発生する事に着目し、

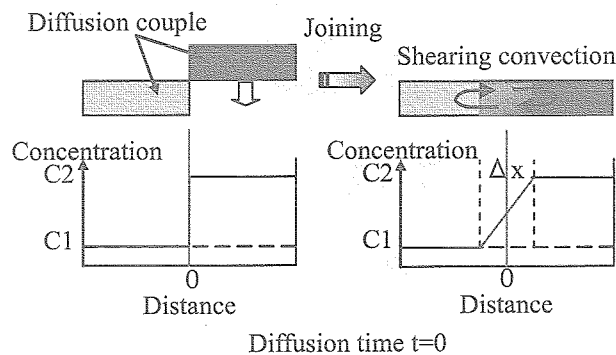


Fig. 5 Schematic figure of the effect of shearing convection.

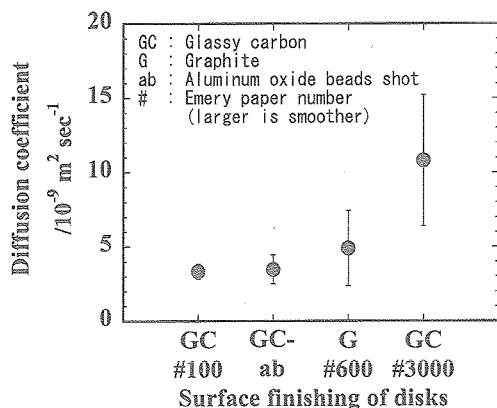


Fig. 6 Relation between the diffusion coefficient and the roughness of disk surface.

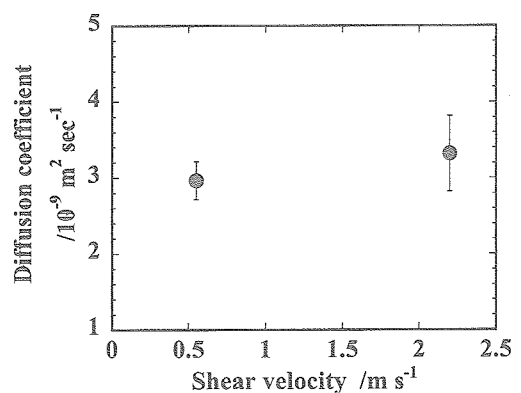


Fig. 7 The relation between the diffusion coefficient and the shear velocity.

拡散保持時間 t を大きくとることにより、その影響を小さくする可能性を考えた。このため、我々は拡散保持時間をパラメータとし、拡散係数の測定値に対する拡散保持時間依存性について実験を行った。

3. 拡散実験

3.1 試料作製

今回の実験では拡散保持時間をパラメータとして十分に長くとるため、実験拡散対試料は従来よりも長く片側 30 mm (接合時 60 mm) とした。また、実験試料は Ag -Ag_{0.95}Au_{0.05} とし、グラファイト製の $\phi 1$ mm の鑄型に鑄込んで各拡散試料片を製作した。特に Ag_{0.95}Au_{0.05} については、あらかじめその組成の母合金を作製してから $\phi 1$ mm の鑄型へ鑄込んだ。図 8 に試料の鑄込み方法のセットアップ図を示す。

まず、母合金を入れたグラファイト製の鑄型を石英管内に配置し真空引きを行い、それを電気炉により融点より 100°C 程高く加熱保持して試料を熔融させた。そして、試料熔融後、石英管内に配置しておいた石英棒によりつば内に試料を鑄込んだ。試料の凝固時の偏析を可能なかぎり小さくし均一な組成の試料を得るため、鑄込み後すぐに電気炉から取り出して石英管ごと浸水させ急冷を行った。さらに実験時には、試料組成の均一化のため、試料の接合前に実験温度において 1 時間程度の保持を行った。

3.2 実験条件

今回行った実験条件を表 1 に示す。実験温度を 1300 K と 1500 K の 2 条件、拡散時間を 240 ~ 25200 sec にわたって実験を実施した。各温度、各時間について最低 4 点データを取得した。

3.3 試料分析 (濃度プロファイル取得)

今回の実験で使用したシアーセルは、一式のつばで 2 対の拡散対の実験が可能であり、一回の実験につき 120 点 (セル 60 枚 \times 2 試料分) の分析試料が発生する。拡散実験では、拡散係数を得るためにそれらすべての組成分析が必要であり、また、測定誤差を小さくするために同一条件において繰り返しデータの蓄積が必要である。しかし、このような多量の試料の組成分析を行うには時間がかかるため、これがデータ取得上の律速となっていた。

そこで試料前処理の簡素化および分析時間の短縮のため、我々はプレス機を使用した試料折り畳みによる濃度の均一化方法を提案し、蛍光 X 線分析法 (EDX) と組み合わせた分析方法を検討した [4]。図 9 に折りたたみによる試料前処理法を示す。

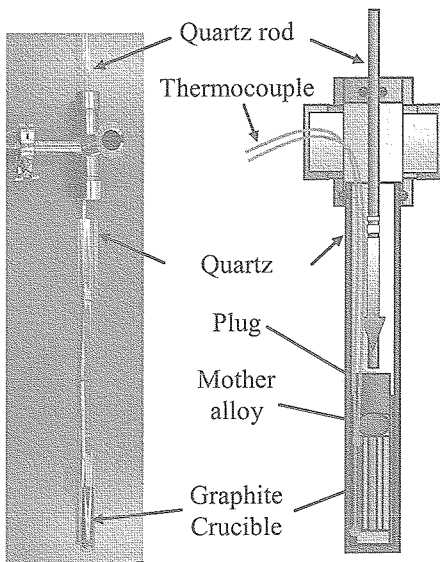


Fig. 8 Mould method for the preparation of diffusion sample.

Table 1 Experimental condition.

Diffusion temperature	1300 K and 1500 K
Diffusion time	240 ~ 25200 sec
Composition	Ag (upper) - Ag _{0.95} Au _{0.05} (lower)
Atmosphere	Ar gas 1 atm
Temperature profile	temperature difference $\Delta t = 15$ K (Upper is higher)

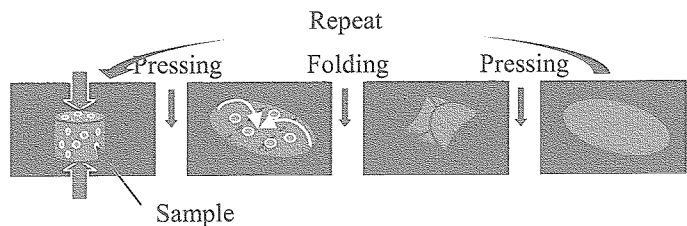


Fig. 9 Pressing and folding method.

この方法による分析精度を確認するため、同一試料について蛍光X線分析（EDX）とICP分析を実施し、それらの結果を比較した。表2にその結果を示す。Au5 at %を含んだ試料を用いた両方法での分析値の差は約0.2 at %であり、前処理法と分析法の選択に特に問題がないことを確認した。

Table 1 Comparison between the analyzed result of EDX and that of ICP.

Sample	EDX (at%)	ICP (at%)	Difference(at%)
A	3.01	2.98	0.03
B	5.35	5.56	-0.21

従来は1実験分（2拡散対分）の試料の分析に約16時間費やしていたが、現在では、分析試料自動交換機構付のEDXの導入も相俟って、約9時間で分析が可能となっている。

4. 実験結果および考察

図10に得られた溶融Ag中のAuの濃度プロファイルの一例を示す。これは実験温度1300 K、拡散保持時間10800 secで行った結果である。○印は実験値、実線はFickの第二法則の解析解である誤差関数で実験値へ最小自乗法によりフィッティングした結果である。実験値は誤差関数に良く一致し、この条件の溶融Ag中のAuの拡散係数として $2.18 \times 10^{-9} \text{ m}^2/\text{sec}$ が得られた。

図11に溶融Ag中のAuの拡散係数の拡散保持時間依存性を示す。図中の線は見方の指針を示す。今回の結果より実験温度1300 K、1500 Kともに得られた拡散係数は、拡散保持時間依存性を示し、拡散保持時間の延長とともに値は減少傾向を示すことが明らかとなった。また、約10800 sec以上の拡散保持時間において、拡散係数はそれぞれある一定の値に収束することが明らかとなった。このとき得られた拡散係数は1300 Kでは $2.22 \times 10^{-9} \text{ m}^2/\text{sec}$ 、1500 Kでは $3.15 \times 10^{-9} \text{ m}^2/\text{sec}$ であった。拡散保持時間を充分長く取ることにより接合時に起こる試料の擾乱の影響を最小限とした拡散係数が得られることが明らかとなった。

地上において液体試料中に発生した流れは、拡散対を混合させ、得られる拡散係数は拡散保持時間とともに増加することが考えられる。しかし、今回の実験結果では拡散保持時間を長く取ったとき、拡散係数は保持時間と関係なく一定値に収束した。これは実験条件として試料上端の温度を試料下端よりも約15 K高く保持し、さらに相対的に密度の低いAg試料を密度の高い $\text{Ag}_{0.95}\text{Au}_{0.05}$ 試料よりも上部に配置したことにより、対流の発生・促進が抑制されたためと考えられる。

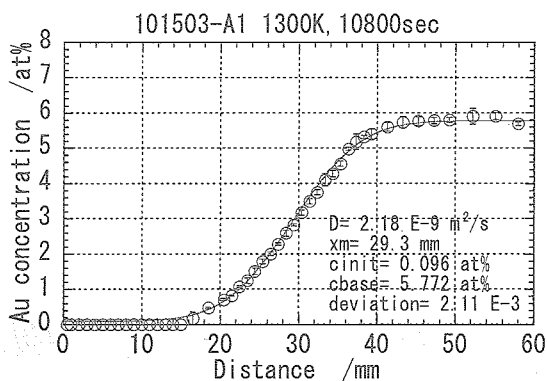


Fig. 10 The typical example of the concentration profile.

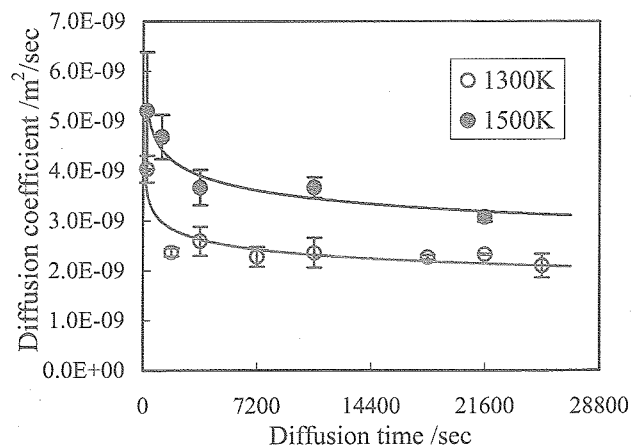


Fig. 11 The diffusion time dependence of diffusion coefficient.

5. 結 論

今回モデル試料として Ag-Ag_{0.95}Au_{0.05} を用いて、実験温度 1300 K, 1500 K における溶融 Ag 中の Au の拡散係数の測定実験を行い、拡散係数の拡散保持時間依存性を得た。この結果から長時間の拡散保持時間をとることにより、シアー対流の影響を限りなく排除した条件で拡散係数の測定ができることが明らかとなった。今回の実験条件では約 10800 sec 以上の拡散保持時間を取ることで真の値に近い拡散係数を得ることができ、実験温度 1300 K では $2.22 \times 10^{-9} \text{ m}^2/\text{sec}$, 1500 K では $3.15 \times 10^{-9} \text{ m}^2/\text{sec}$ を得た。

参 考 文 献

- [1] M. Uchida, Y. Watanabe, S. Matsumoto, M. Kaneko, T. Fukazawa, T. Masaki and T. Itami: Proc. of 22 nd Japan Symposium on Thermophysical Properties (2001) 437-439.
- [2] Y. Watanabe, T. Fukazawa, S. Matsumoto, M. Uchida and T. Itami: J. Jpn. Soc. Microgravity Appl., Vol. 19, Supplement (2002) 14.
- [3] S. Matsumoto, F. Otsubo, M. Uchida and T. Itami: Proc. of 22 nd Japan Symposium on Thermophysical Properties (2001) 440-442.
- [4] T. Fukazawa, Y. Watanabe, M. Uchida, T. Masaki and T. Itami: Proc. of 23 rd Japan Symposium on Thermophysical Properties (2002) 15-17.

Current status of the development of shear cell technique in ground base research and towards JEM on ISS

Tadahiko MASAKI^{*1}, Tomoharu FUKAZAWA^{*1}, Satoshi MATSUMOTO^{*1},
Toshio ITAMI^{*2} and Shinichi YODA^{*1}

Abstract: The microgravity condition is one of the ideal conditions for the measurements of diffusion coefficients in high temperature melts because of the absence of convection in the liquid sample. The many kinds of experimental techniques, such as, the long capillary method and the shear cell method, have been devised in the ground base research for the measurement of diffusion coefficient in such high temperature melts. Recently, the shear cell technique coupled with the microgravity condition was applied to the measurements of high temperature metallic melts. This technique enables us to measure the diffusion coefficient with high precision. In this paper, a brief discussion is given for the trends of previous diffusion experiments in space performed by Japanese researchers. Recently, Japanese space agency, JAXA, is developing the shear cell technique for the future space experiments in JEM. The current status of the development of our shear cell technique is summarized and new results are presented for typical experiments on the ground by using test samples, for example, liquid silver-gold alloys.

Keywords: shear cell, diffusion coefficient, liquid metals

1. INTRODUCTION

The transport properties in molten states are one of the important features for the understanding of the liquid nature of materials and also are important for the industrial processing such as the crystal growth of semiconductors. Especially, the diffusion coefficient is directly related to the mass transport in liquids. Therefore, the many efforts have been devoted to the developments of measurement techniques [1]. The tracer method is the most popular way for the direct measurement of diffusion coefficient. Two kinds of materials (a diffusion pair) are contacted in a vessel and the diffusion sample is formed. The time development is investigated for the tracer concentration profiles in this sample. Several kinds of elements are selected for the tracer of diffusion depending on the aim of measurements. The isotopes are selected as the tracer of the measurements of self-diffusion coefficient. The impurity atoms are selected as that of the impurity diffusion coefficient. In the case of inter diffusion coefficient, the analysis of the time development of component concentration is performed for a diffusion pair whose initial concentration is different between constituent pieces.

The long capillary method has been widely used because of its simplicity on the experiments and the data analysis. The sample materials are contained in a narrow capillary whose diameter is 1–2 millimeter. Frequently, the diffusion couple is selected as the initial configuration of diffusion. The diffusion couple is composed of two kinds of sample materials with equal length which is connected at the center of capillary. Usually, one of sample material is enriched by the tracer elements. The change of concentration is described in terms of the diffusion equation as shown in following equation,

$$\frac{\partial c}{\partial t} = D \frac{\partial^2 c}{\partial x^2}, \quad (1)$$

* 1 Japan Aerospace Exploration Agency, Institute of Space and Astronautical Science, ISS project office 2-1-1 Sengen, Tsukuba-city, Ibaraki, 305-8505 Japan
* 2 Graduate School of Science, Hokkaido University Kita 10 Nishi 5, Sapporo 060-0810, Japan

, where c is the concentration of tracer, t is the time, x is the distance and D is the diffusion coefficient.

Since this method is applicable to various kinds of materials, the many variations of long capillary method have been developed. Ozelton and Swalin [2] applied this technique to the measurements of self-diffusion coefficient of liquid sodium at the constant volume and the constant pressure. After the diffusion experiments, the profile of sodium isotope distribution was fitted to the error function which is the analytical solution of equation (1) corresponding to the step function as the initial concentration profile. In addition to the diffusion couple method, the several kind of the initial configuration is selected, for example, a small piece of tracer is placed only at the end of capillary, which corresponds to the delta function as the initial concentration profile. Larsson *et al.* [3] measured the self-diffusion coefficient of liquid gallium with the use of this configuration.

The long capillary method is the most conventionally employed for the diffusion experiments in liquids. However, it is a fact that this method is easily affected by the convection under the normal gravity condition. For the suppression of convection in liquid samples, the sample is contained in a narrow capillary. Nevertheless, the convective flow in the liquid sample spoils the concentration profile of tracer in the diffusion sample on the ground. Figure 1 shows the comparison of self-diffusion coefficients of liquid tin measured on the ground and those under microgravity. The diffusion coefficients measured under the normal gravity are widely scattered depending on the data source [4–8]. It can be easily seen that the measured diffusion coefficient is disturbed by the convection, which is remarkable at the higher temperature. The measurements of diffusion coefficient under microgravity were performed by Froberg *et al.* [9], Itami *et al.* [10] and Yoda *et al.* [11]. The microgravity diffusion data of them shows a common temperature dependence without large data scattering. This indicates that the microgravity provides an ideal circumstance for diffusion measurements with no convection. Another point we must consider is that the long capillary method experiences the melting and solidification process during the diffusion experiment. The concentration profile of tracer in the long capillary is disturbed easily by the segregation or the volume change on melting and solidification of liquid sample.

If the liquid diffusion couple can be connected into one piece and separated into many pieces of segments at temperature higher than the melting temperature, it is not necessary to be bothered about the volume change or segregation on melting and solidification. The shear cell technique was innovated in order to eliminate these experimental error sources. The shear cell is constructed from the thin disks which can rotate co-axially. A few small holes are prepared around the center axis to contain the sample. The positions of holes are designed correspondingly to the rotation angle of each disk. The liquid sample can be joined and separated with the rotation of each disk. Nachtrieb *et al.* [12, 13] developed the shear cell for the measurement of self-diffusion coefficient of liquid mercury and gallium. Barras *et al.* [14] measured the diffusion coefficient of liquid thallium. Bruson *et al.* [7, 15] measured diffusion coefficients of tin isotope, antimony, silver and gold atom in liquid tin and in liquid copper respectively. In the early stage, the shear cell was made of metal. Then, the shear cell was made of sintered graphite and sintered boron nitride and was applied to the wide variety of liquid metals. Recently, the shear cell method was applied to the measurement of diffusion coefficient of GaSb [16] and aluminum in liquid gallium and indium [17].

Since 1970th, the microgravity condition has been regarded as an ideal condition for the measurement of diffusion coefficient because of the absence of convective flow due to the weightless condition. Ukanwa [18] performed the first diffusion experiments in space on the Skylab in 1973 and showed us the efficiency of microgravity condition. Reeds *et al.* [19] performed the diffusion experiment of gold in liq-

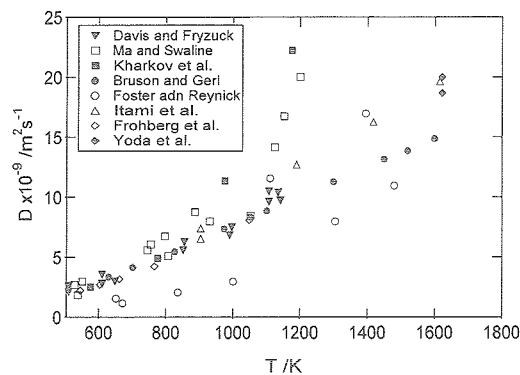


Fig. 1 Self-diffusion coefficient of liquid tin. Data of Davis and Fryzuck[8], Ma and Swaline[5], Kharkov *et al.*[4], Bruson and Gerl[7] and Foster and Reynick[6] are measured in the normal gravity. Data of Froberg *et al.*[9], Itami *et al.*[10] and Yoda *et al.*[11] are measured in the microgravity.

liquid lead under the microgravity on the Apporo-Soyuz. Minster *et al.* [20] measured the impurity diffusion coefficient of copper in liquid lead under the microgravity condition. Frohberg *et al.* performed the pioneering work of diffusion research in space in the space shuttle missions of SL-1 [9], D-1 [21] and D-2 [22,23] and showed that the diffusion coefficient in liquids can be measured with high accuracy under microgravity. Malmejac *et al.* [24, 25] measured the thermomigration coefficient of cobalt in liquid tin with the use of shear cell in the SL-1 mission, which was the first shear cell experiment under microgravity. Diffusion experiments performed in the space shuttle and sounding rocket were summarized in the reviews [26, 27]. Matthiesen *et al.* [28] tried to measure the impurity diffusion in liquid germanium on the space shuttle in 1997. Smith *et al.* [29] measured the diffusion coefficient of many kinds of liquid metals on the Russian space station, MIR. Praizey and Frohberg [30, 31] measured the diffusion coefficient of metallic alloys by the use of shear cell on the retrievable capsule, FOTON in 1999.

In Japan, the diffusion experiments under microgravity were performed both in the space shuttle and in the sounding rocket. Especially, the sounding rockets have played an important role for Japanese diffusion experiments under microgravity. Uchida *et al.* [32] measured the mutual diffusion of PbTe-SnTe on the TEXUS26 in 1990, TEXUS29 in 1992 and TR-IA4 in 1995. Itami *et al.* measured the isotope diffusion of liquid germanium [33], isotope diffusion of liquid lithium [34]. The shear cell method coupled with the microgravity condition is the best way for measuring the diffusion coefficient in high temperature liquids. The shear cell experiment under microgravity was performed by Yoda *et al.* [35] on the TR-IA sounding rocket in 1996 for the measurement of isotope diffusion of liquid germanium. In Japan, the first diffusion experiment under long duration microgravity was performed on the SL-J mission by Dan *et al.* [36] in 1992. Nakata *et al.* [37] measured the diffusion coefficient of liquid InSb in the D-2 mission. The systematic investigation of diffusion phenomena under microgravity have been performed in the space shuttle in MSL-1 international mission by Japanese group. Itami *et al.* [10] measured the self diffusion coefficient of liquid tin with the use of the long capillary method at the temperatures higher than Frohberg's experiments. Uchida *et al.* [38] measured the mutual diffusion coefficient of PbTe-SnTe quasi binary semiconductor melts. Yoda *et al.* [11] have refined the shear cell technique and improved its reliability for the long duration microgravity experiments. The improved shear cell was tested to the experiment of self diffusion in liquid tin and mutual diffusion in PbTe-SnTe, for which the long capillary experiments were performed by Itami *et al.* [10] and Uchida *et al.* [38] respectively on the same microgravity mission (MSL-1). Yamamura *et al.* [39] measured the impurity diffusion of silver ion in molten salts with the use of the electro-chemical method.

The shear cell technique is powerful especially for the measurement of diffusion coefficient on sounding rocket experiments. The start and the end of diffusion can be controlled mechanically by the shear cell technique. Therefore, the short duration of microgravity, usually six minutes, on the sounding rocket can be fully used for the diffusion time without the problem of convection. The microgravity duration of sounding rocket is rather short for the precise measurements of the diffusion coefficient, but enough its the measurement with acceptable accuracy (10 % –20 %). In 1998, Itami *et al.* [40] and Kinoshita *et al.* [41] performed the measurement of diffusion in liquid alloys and molten semiconductors respectively with the use of refined shear cell. In these experiments, the glass seal technique [42] was developed for the prevention of the sample from evaporation.

The shear cell for the space experiment was made of sintered boron nitride. Boron nitride is easy to make a complicate shape but the finishing accuracy of machine work is limited by its fragility. Therefore the 2 millimeter diameter of sample must be accepted for the feasible connection of diffusion couple. This sample diameter of previous shear cell for the space experiments was somewhat large to prevent the convection under the normal gravity on ground. Recently, the many kinds of novel crucible materials have been developed. The precision of finishing of crucibles can be extremely improved enough to make the refined shear cell whose sample diameter is less than 1 millimeter; the considerably precise measurement of diffusion coefficient can be performed even on ground. In this paper, the feature of our shear cell is briefly introduced and the results of test experiment are described.

2. TECHNICAL DETAILS OF SHEAR CELL METHOD

The diffusion measurement due to the long capillary method is easily spoiled by the convective flow and the volume change on melting and solidifying the sample. The shear cell method has developed in order to overcome these problems. In the shear cell methods, the liquid diffusion sample is contained in the long and narrow space similarly to the case of long capillary method. The sample space is made of the pile of thin holes in the disks. Each disk has a hole for a center rod at the center and two or three sample holes around the center hole. Each disk can be rotated separately in order to form liquid columns of the sample for diffusion experiments at the start of diffusion and divides the liquid sample into small piece for the concentration analysis at the stop of it.

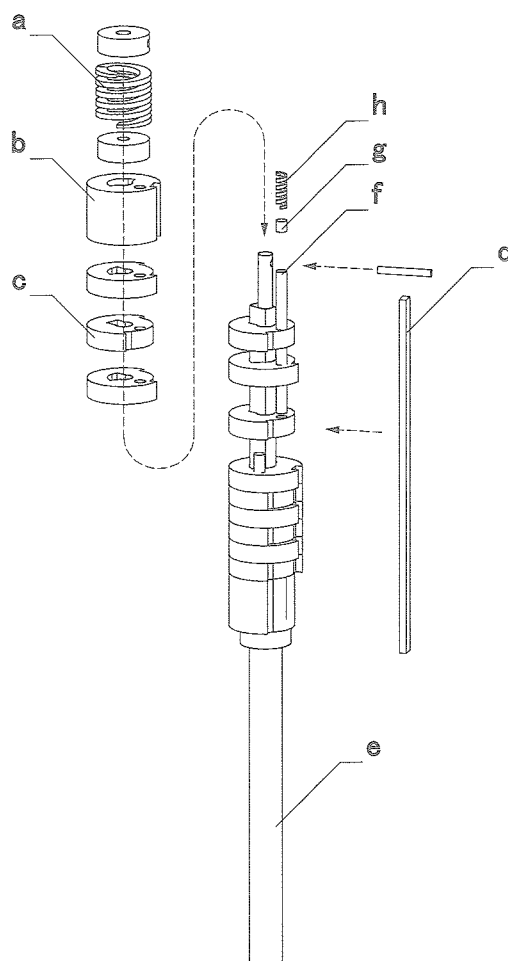


Fig. 2 Schematic figure of shear cell
 a: carbon spring; b: end part; c: disk crucible; d: fixed rod; e: center rod;
 f: diffusion sample; g: carbon rod; h: graphite spring.

The shear cell technique is now being developed in JAXA for the ISS experiments by using the $\text{AgAg}_{0.05}\text{-Ag}$ diffusion couple as a test sample. The shear cell assembly developed in JAXA was composed of more than twenty disks for crucibles, two end disks, a center rod and a crucible holder, as can be seen in figure 2. The same one millimeter was taken as the thickness of disk for the crucible and the diameter of sample hole respectively. The disk parts were made of glassy carbon for which the extremely fine machine work can be applied and other parts were made of sintered carbon. The center rod was made of mullite because of its low thermal conductivity. The samples, which was cast into the rod shape beforehand, were installed in the shear cell together with carbon springs and carbon rods whose diameters were same as those of sample. The typical length of the diffusion couple was 60 millimeters. The springs and rods were placed at the both ends of sample in order to compensate the volume change of sample on heating process particularly on melting and in order to avoid any void formation in the liquid diffusion sample. The experimental inserts were the shear cell, the heater and the ceramic tube which separates the shear cell from the air atmosphere. The heater of sample was made of pyrolytic carbon covered by pyrolytic boron nitride. The experimental inserts were introduced into the experimental chamber with X-ray image observation system. This facility is the ground test model of the Advanced Furnace for microgravity Experiment with X-ray radiography, AFEX, for the Japanese Experimental Module, JEM for the ISS (International Space Station). All of parts of experimental inserts are made of ceramics materials except for the diffusion sample. Therefore, the direct “*in situ*” observation of the connection and the division of liquid sample on the shear cell operation can be observed by the X-ray radiograph.

The resolution of X-ray radiograph is about 0.1 millimeter. A motor was fixed at the bottom of the experimental insert and was connected to the center rod of the shear cell assembly. The W-Re thermocouples were installed at the side of shear cell for the temperature measurement. The observation chamber and experimental inserts are evacuated and filled with high purity argon gas.

The sample in the shear cell was heated by the ceramic heater. The melting behavior was observed by the use of X-ray image. Following the melting of sample, the center rod was rotated by the motor at the bottom of the experimental insert and the each piece of the diffusion couple which had been separated at the initial configuration was joined into one liquid column, the liquid diffusion couple. The joining into the liquid diffusion couple was also observed by the X-ray image.

After the appropriate diffusion time was progressed, the center rod was rotated to the opposite direction and the liquid diffusion sample was divided into small pieces. Figure 3 shows the images of diffusion sample at each experimental stage due to the X-ray radiograph. Then, the shear cell assembly was cooled and the tracer concentration of each sample was analyzed. The dimension of divided diffusion sample was one millimeter diameter and one millimeter length. The shape of each divided sample was changed into thin plate of about 8mm diameter by the repetition of pressing and folding for the measurement of average concentration of overall piece by the X-ray fluorescence analysis.

Since the liquid diffusion sample is created only in the diffusion time by the mechanical operation for the shear cell method, the obtained diffusion coefficients become free from the experimental problem of long capillary method such as the proceed of the diffusion on heating and cooling process and segregation. However, the inherent problems to the shear cell method appear, for example, the miss alignment of diffusion sample and the additional flow induced by the rotation of disks. Our shear cell assembly was contrived in order to minimize the experimental error caused by these inherent problems.

For the solution of the first problem, the accuracy of machine work for the shear cell crucible was improved with the use of novel ceramic material. The X-ray radiography, which was installed to observe the condition of sample on the diffusion experiment, was also valid. If the misalignment of diffusion couple exceeds ten percent of sample diameter, the observed diffusion coefficients are three percent smaller than the exact value, which was evaluated from the numerical simulation [43]. Our shear cell was made of glassy carbon (Niss-

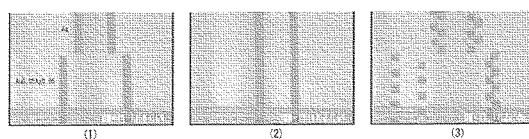


Fig. 3 The X-ray image of Diffusion sample in the shear cell
(1): Before joining; (2): Connected; (3): Divided.

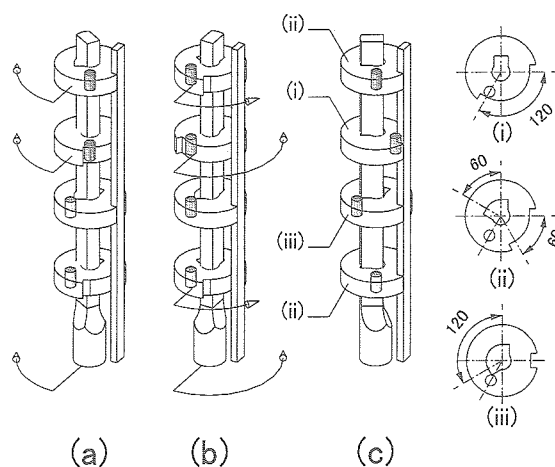


Fig. 4 The mechanism of shear cell.
(a) The rotation for the sample joining. (b) The rotation for the sample division.
(c) The divided state of sample. Arrows indicate the direction of rotation. The disks are separated for the visualization of the mechanism in the drawing. Each sample position is determined due to the rotation direction of center rod, inner arc at the center of disk, outer arc at the rim of disk, position of sample and fixed bar. The degrees of inner and outer arcs restrict the rotation angle of disks.

inbo Industrial Inc.), which is a very hard material. The glassy carbon provides the fine and accurate machinery products whose inaccuracy is less than 1 micrometer. It was confirmed that the misalignment of diffusion sample in our experiments was less than 0.1mm which was smaller than the resolution of X-ray radiography. The error derived from the misalignment was sufficiently negligible.

The second problem is unavoidable for the shear cell method. The rotation of cell added the drag force to the liquid at the contact with the moving disk and a pair of small vortex flow occurs on the joining of liquids. Therefore, the step function of tracer distribution as the initial tracer distribution is destroyed because the small amount of volume exchange occurs between each liquid piece of diffusion couple. This error of concentration in the initial stage provides additional contribution of errors to the evaluation of true diffusion coefficient. The contribution of this problem can be negligible if the diffusion time is sufficiently long. The same situation occurs on the division of liquid sample. The sample division are classified into two cases depending on the design of shear cell; one is a sequential division and the other is a simultaneous one. Each of these patterns has its merits and demerits. In the case of sequential division, the flow pattern in the sample is rather simple since the flow is limited only at the cutting part and this flow part moves sequentially; the finish times of diffusion are different between the first divided part and last one. In the case of simultaneous division, it is not necessary to be worried by the delay of cutting time. But we must be careful for the fact that the flow pattern in the sample is rather complicated. In our shear cell, the latter pattern is selected, i.e. the sample is divided simultaneously. The shear cell disk is constructed of three types of disk which possesses the cut part at the rim and the center hole which can be seen in figure 4. The angles of cut parts and position of sample holes correspond to the rotation angle of disk. The liquid diffusion sample can be joined or divided by the rotation of center rod in the direction of clockwise and counter clockwise respectively. Each disk is rotated simultaneously and is stopped at the appropriate position for the joining and the division due to the combination of cut angle of rim on disks and the fixed rod, which can be seen in figure 4.

3. EXPERIMENTAL RESULTS AND DISCUSSIONS

The Ag-Au alloy was selected as the test material for the verification of the operation of our shear cell. It is well known that the silver and gold are inert materials and both are easy for handling. This system has another merit for the diffusion experiments judging from the analysis of concentration of diffusion sample. The phase diagram of Ag-Au system shows a typical solid solution system whose liquidus line and the solidus line are quite close. Therefore the segregation in the solidified diffusion sample is kept to be sufficiently small. This merit allows us that the concentration profile can be analyzed with the sufficient accuracy by the conventional X-ray fluorescence analysis for the solidified samples.

The diffusion couple was consisted of pure silver and silver-gold alloy in which five atomic percents of gold was contained. Each sample was cast into the narrow rod which was 1 millimeter diameter and 30 millimeter length. The end faces of samples were finished to be flat by the fine polisher for the optical fiber. The diffusion experiments were performed at the temperature of 1300K, which is 56 K higher than the liquidus temperature. The concentration profiles in the solidified samples were determined by the X-ray fluorescence analysis.

In the ideal case, the concentration profile of gold atom in the sample studied should obey the error function, which is the analytical solution of the diffusion equation for the diffusion couple and is given as follows:

$$\frac{2(c(x,t)-c_1)}{c_2 - c_1} = 1 - \text{Erf}(Y) \quad (2)$$

where c_1 and c_2 is the concentration of tracer in the diffusion couple at the start of diffusion. The error function, Erf , is defined as follows:

$$\text{Erf}(Y) = \frac{2}{\sqrt{\pi}} \int_0^Y \exp(-y^2) dy \quad (3)$$

The concentration profiles obtained from experiments are in good agreement with equation (2), which is shown in figure 5. The diffusion coefficient of gold atom in liquid silver was evaluated by the least square fitting of experimental data to this analytical solution (equation (2)).

The diffusion experiments were performed with the variation of the duration of diffusion in order to clarify the magnitude of error due to the joining the liquid. The duration of diffusion was varied from 240 seconds to 25200 seconds. From this variation of diffusion time, the diffusion coefficients obtained from shear cell experiments strongly depend on the duration of diffusion. The diffusion coefficient for the short duration was 50 % larger than for the sufficiently long duration. This is clearly derived from the initial disturbances due to the

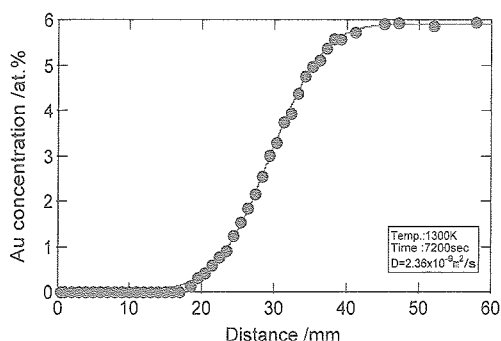


Fig. 5 Typical diffusion profile of Ag-Au_{0.05}Ag_{0.95} diffusion couple with the use of shear cell. The solid circle represents the experiment at 1300K with the diffusion time of 7200 s. The solid line shows the solution of Fick's second law with $D = 2.36 \times 10^{-9} \text{ m}^2/\text{s}$.

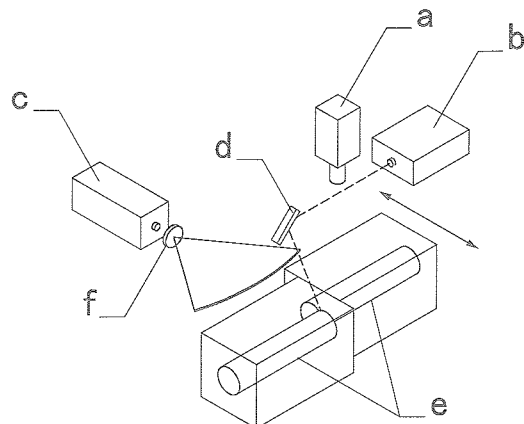


Fig. 6 Schematic figure of the apparatus for the observation of shear flow.

(a): video camera; (b) UV laser for the coloring the photochromic dye; (c): Argon laser; (e): observation cell(acryl resin); (f): cylindrical lens. The cylindrical vacancy of (e) is filled with the silicon oil together with particles and the dye.

joining of the liquid diffusion sample on the shear cell operation.

Concerning the initial disturbance of the shear cell technique, direct observation experiments were carried out with the use of silicon oil as a model fluid. The properties of fluid mechanics, for example, kinetic viscosity, the scale of model cell and the velocity of cell movement, were determined by simulating the hot liquid sample in the shear cell. The flow pattern observed were classified by the non-dimensional fluid parameter i.e. Reynolds number, $Re = ud/v$, where u , d and v are the shearing speed of cell, the diameter of sample and the kinematic viscosity respectively. In the diffusion experiments of liquid silver alloys, the Re is equal to 1.8 where $u = 0.554 \text{ mm/s}$, $d = 1.0 \text{ mm}$ and $v = 0.396 \text{ mm}^2/\text{s}$. The Re was varied from 0.2 to 110 due to the change of shearing speed and the viscosity of silicon oil. The motion of model fluid was observed by the photochromic dye [44, 45] in addition to the tracking of the particle tracer. The observation system is shown in figure 6. The same kinds of experiments are reported by several authors, though most of them used particles as a marker of flow. This experiment is the first to use the photochromic dye as a marker of shear flow for the shear cell. The density of colored fluid and others are not different in the case of photochromic dye method. It is not necessary to worry about the sedimentation or the buoyancy of tracer particles. Furthermore, it is available to mark only the fluid at the contact of diffusion couple. The flow pattern of each time step is shown in figures 7 and 8. It can be seen that the small vortex flow was induced by the drag force given by the movement of the cell. The photochromic dye clearly indicated the trajectory of fluid motion at the contact of liquid diffusion couple.

This trajectory was regarded as the ridge of area of liquid exchange between the samples of diffusion couple. Figure 9 shows the dependence of penetration length, L on Re .

Under the condition of the Re of diffusion experiments of liquid silver alloys, which is about 10, the influenced area of flow was estimated to be within the adjacent part to the interface of the joining part. The influenced length was less than 20 % of the sample diameter.

The time dependence of observed diffusion coefficients can be explained by the result of this model fluid experiment qualitatively, as shown in figure 10. The enlarged diffusion coefficients due to the initial flow on joining are evaluated by the numerical simulation with the change of the penetration length, L . The initial concentration of disturbed area would be evaluated as the interpolation of linear function of each concentration of diffusion couple. The exact diffusion coefficient of gold in silver was assumed to be $2.24 \times 10^{-9} \text{ m}^2/\text{s}$. This value was obtained from the average value of experiments whose duration of diffusion was sufficiently long. Figure 10 shows the comparison of experimental data with results of numerical simulation. In the case of L equal to the sample diameter, the result of simulation is in good agreement with the experimental result. The L evaluated from this numerical simulation is five times larger than that of model fluid experiments. The quantitative difference of L between the actual diffusion experiment and model fluid experiment may be derived from the wetting of sample to the shear cell. The additional experiments should be performed for the quantitative estimation of L from model fluid experiments which simulate also the wetting condition. Nevertheless, the observed diffusion coefficients became constant when the diffu-

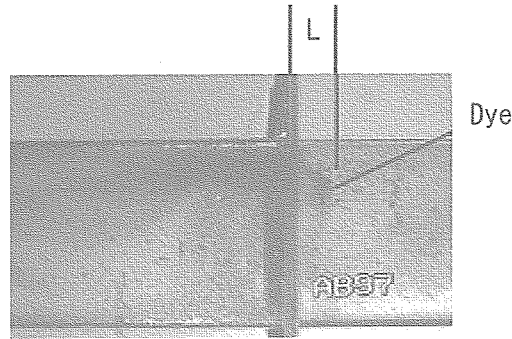


Fig. 7 Video image of induced flow on joining two liquid columns by using the photochromic dye

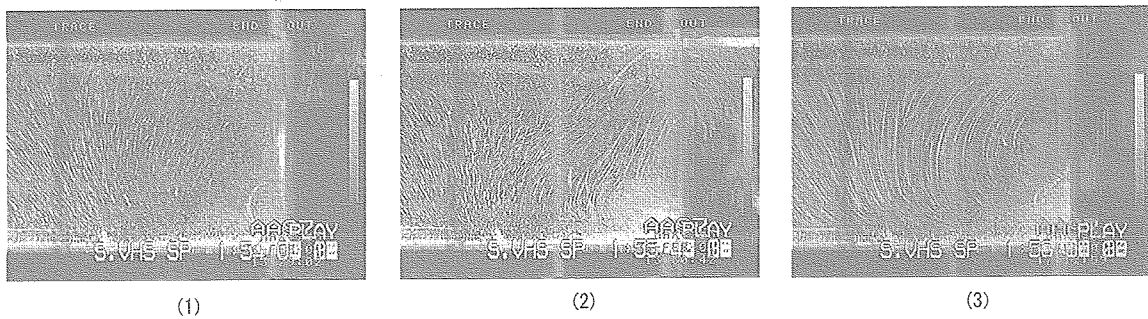


Fig. 8 Video Image of flow pattern (1): Beginning of joining; (2): Intermediate state; (3): End of joining

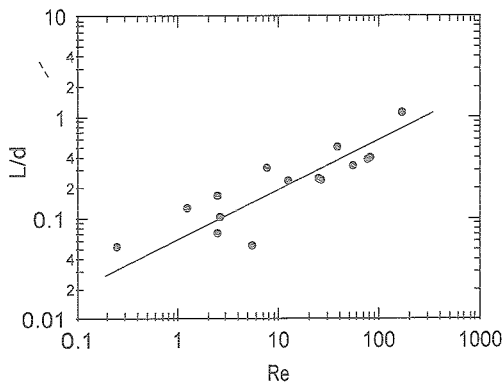


Fig. 9 Relation between L/d and Re for the model fluid simulation; L : penetration depth; d : diameter of hole in the shear cell disk; Re : Reynolds number.

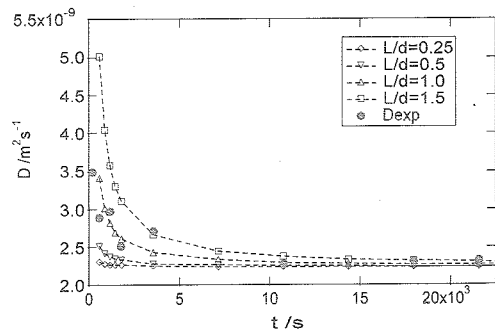


Fig. 10 The time dependence of the observed diffusion coefficient. Closed circle: experimental data; open marks: numerical simulation.

sion time longer than 10800 sec, as shown in figure 10. Hence, the disturbance of initial disturbance of flow on joining can be negligible if the diffusion time is sufficiently long.

The same kind of flow is also induced by the cutting process and the stream of flow is much more complicated. Nevertheless, the effect on diffusion coefficient can be regarded to be much smaller than the former case because of following two reasons. The first one is that the concentration differences between the divided samples are small at this stage and, therefore, the concentration change due to the liquid exchange may be small. The second one is that the small vortex flows induced by the cutting process is limited just in the neighborhood of interfaces of divided samples. Therefore, the influence of cutting process dose not exceed the length of divided sample and the error due to this cause may be negligible.

Finally the discussion is focused on the influence of the convective flow on the diffusion coefficient measured by the shear cell. If the convection occurs in the sample, the mixing of diffusion couple is enhanced. Therefore, the observed diffusion coefficient increases

depending on the diffusion time. Nevertheless, the experimental results show that the diffusion coefficient becomes independent on the diffusion time in the case of the long diffusion time. The diffusion coefficient obtained, $2.24 \times 10^{-9} \text{ m}^2/\text{s}$, for liquid $\text{AgAu}_{0.05}\text{-Ag}$, is slightly lower than the experimental value by Gupta, which is $2.46 \times 10^{-9} \text{ m}^2/\text{s}$ [46]. The experimental errors of long capillary method, i.e. the undesirable diffusion on heating and cooling process and the segregation on solidification, tend to increase the measured diffusion coefficient. The shear cell method adopted here is advantageous for the removal of these errors. In the present experimental configuration, the density of liquid silver in the upper position is lighter than that of silver-gold alloy in the lower one. Additionally, the temperature of upper part was kept to be about five degrees higher than that of lower part in order to prevent the convection. The present configuration might suppress the occurrence of convection in the liquid sample.

4. THE CURRENT STATUS OF THE SHEAR CELL FOR THE MICROGRAVITY EXPERIMENTS ON ISS

The shear cell, which is now being developed in JAXA, is applicable to the microgravity experiment without any change of basic design. The shear cell with the similar design has been successfully applied to the microgravity experiments [11, 35]. Currently, the experimental insert of shear cell is being developed for the measurement of self and impurity diffusion in liquid germanium, which is to be performed as microgravity experiments in JEM. The furnace, which is named as the gradient heating furnace, GHF, has three heaters in the evacuated chamber and the available maximum temperature is around 1870 K. The GHF is developed for the high temperature experiment with temperature gradient such as the crystal growth of semiconductors. The GHF is also applicable to the isothermal experiment for the optimization of furnace configuration. The design of experimental insert for the shear cell experiment in JEM is same as that of the grand base experiment, which is consisted of shear cell covered with a tube and a fitting part to the furnace, thermocouple and motor for cell rotation. The test experiment will be performed in the GHF by using the test model of experimental insert in the near future.

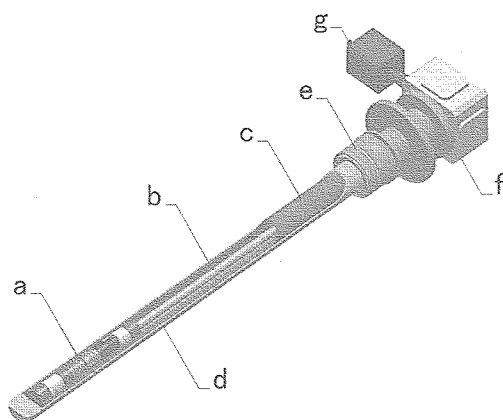


Fig. 11 Experimental insert for the GHF.
a: shear cell assembly; b: center rod; c: shear cell support; d: metal tube;
e: fitting part of GHF; f: interface box; g: motor.

5. CONCLUSION

The experimental results of simulation of fluid motion for the shear cell are in good agreement with the numerical simulation whose initial mixing length is equal to the capillary diameter. The diffusion coefficient can be measured by the use of present shear cell if the diffusion time is sufficiently long; in the case of liquid metals, longer than 2 hours (10800 sec). In the case of this experiment, the convective flow can be regarded to be negligible since the density difference between the upper part and the lower one properly established to suppress the convection. The shear cell technique is satisfactory for the measurement of the diffusion coefficient with high precision. Nevertheless, the convection in the diffusion sample cannot be avoided completely on the ground for some interesting cases, for example, the measurements of the self-diffusion coefficient just above the melting temperature and the diffusion with the strong temperature depen-

dence. It should be noted that it is the next best method to add the temperature gradient to measure the exact diffusion coefficient. The diffusion coefficient itself should be determined on the isothermal condition. In such cases, the microgravity condition coupled with the shear cell will be the last resort for the measurement of diffusion.

REFERENCES

- [1] M. Shimoji and T. Itami, "Atomic Transport in Liquid Metals", Trans tech publications, Switzerland (1986).
- [2] M.W. Ozelton and R.A.Swalin, Phil. Mag., 153,441 (1968).
- [3] S. Larsson, L. Broman, C. Roxbergh and A. Lodding, Z. Naturforsch., 25a, 1472 (1970).
- [4] E. I. Kharkov, A. P. Zvyaginstsev and G. I. Ohoprienko, Fiz. Metal. Metalloved., 31, 220 (1971).
- [5] C. H. Ma and R. A. Swaline, Acta Met., 8, 388 (1960).
- [6] J. P. Foster and A. J. Reynick, Met. Trans., 4, 207 (1973).
- [7] A. Bruson and M. Gerl, Phys. Rev. B, 21, 5447 (1980).
- [8] K. G. Davis and P. Fryzuck, J. Appl. Phys., 39, 4848 (1968).
- [9] G. Frohberg, K. H. Kraatz and H. Weber, ESA-SP-222, 263 (1979).
- [10] T. Itami, H. Aoki, M. Uchida, A. Sisa, S. Amano, O. Odawara, T. Masaki, T. Oida, H. Oda and S. Yoda, NASA-CP-1998-208868, pp.60 (1998).
- [11] S. Yoda, T. Masaki and H. Oda, NASA-CP-1998-208868, pp.86 (1998).
- [12] N.H. Nachtrieb, J. Chem. Phys., 24, 746 (1956).
- [13] J. Petit and N. H. Nachtrieb, J. Chem. Phys., 24, 1027 (1956).
- [14] R. E. Barras, H. A. Walls and A. L. Hines, Met. Trans., 6B, 347 (1975).
- [15] A. Bruson and M. Gerl, Phys. Rev. B, 19, 6123 (1979).
- [16] G. Muller-Vogt and R. Kossler, J. Cryst. Growth, 186, 511 (1998).
- [17] P. Brauer and G. Muller-Vogt, J. Cryst. Growth, 186, 520 (1998).
- [18] A. O. Ukanwa, M.588 - "Skylab results", NASA-MSFC, 427 (1979).
- [19] R. E. Reeds, W. Uehlhoff and H. L. Adair, NASA-SP412, 1, 367 (1977).
- [20] O. Minster, C. Vahlas, C. Senillou., L. Coudrier, N. Eustathopoulos and P. Desre, 4th European Symposium on "Material Science under Microgravity".
- [21] G. Frohberg and K.H Kraatz, Proceedings of "International Conference on D-1 Results, pp.27, (1986).
- [22] G. Frohberg, "Diffusion in liquids" in "Scientific Results of the German Spacelab Mission D-2", 275 (1995).
- [23] G. Frohberg, K. H. Kraatz, A. Griesche and H. Weber, "Diffusion in metals and alloys: self- and impurity diffusion", in "Scientific Results of the German Spacelab Mission D-2", 288 (1995).
- [24] Y. Malmejac and J. P. Praizey, ESA-SP-222, 147 (1984).
- [25] J. P. Praizey, Int. J. Heat Mass Transfer, 32, 2385 (1989).
- [26] G. Frohberg, "Diffusion and Atomic Transport" in "Materials Science in Space", Sprigner-Verlag, Berlin (1986), pp.93.
- [27] Y. Malmejac and G. Frohberg, "Mass Transport by Diffusion", in "Fluid Sciences and Material Sciences in Space, Springer-Verlag, Berlin (1987), pp.159.
- [28] D. H. Matthiesen and M. L. Kaforey, NASA-CP-1999-209092, pp. 443 (1999).
- [29] R. Smith, X. Zhu, M. C. Tunnicliffe, ESA-SP-454, pp. 887 (2000).
- [30] J.P. Praizey, J.P. Garandet, G. Frohberg, A. Griesche and K.H. Kraatz, ESA-SP-454 "Proceedings of First International Symposium on Microgravity Research and Applications in Physical Science and Biotechnology", 481 (2000).
- [31] J.P. Garandet, G. Mathiak, V. Botton, P. Lehmann and A. Griesche, Int. J. Thermophys. 25, 249 (2004).
- [32] M. Uchida, a thesis for a doctor.
- [33] T. Itami, M. Kaneko, M. Uchida, S. Yoda and T. Masaki, *J. Jpn. Soc. Microgravity Appl.*, 14, 323 (1997).
- [34] T. Itami, M. Kaneko, T. Fukazawa, M. Uchida, S. Yoda and T. Masaki, *J. Jpn. Soc. Microgravity Appl.*, 15, 165 (1998).
- [35] S. Yoda, H. Oda, T. Nakamura, T. Masaki, N. Koshikawa, S. Matsumoto, A. Tanji, M. Kaneko, Y. Arai, K. Goto and N. Tateiwa, *J. Jpn. Soc. Microgravity Appl.* 14, 331 (1997).

- [36] T. Dan, Y. Muramatsu, T. Yamagata, K. Hoshino, Proceedings in “The 7th SL-J Post Flight IWG 6 Month Science Report, pp.12, 1993.
- [37] Y. Nakata, T. Yasunaga and H. Yoshida, “Scientific Results of the German Spacelab Mission D-2”, 309 (1995).
- [38] M. Uchida, M. Kaneko, T. Itami and S. Yoda, NASA-CP-1998-208868, pp.72 (1998).
- [39] T. Yamamura, S. Yoda, T. Oida and T. Masaki, NASA-CP-1998-208868, pp.80 (1998).
- [40] T.Itami, M.Kaneko, T.Fukazawa, T.Masaki, S.Matsumoto, S.Munejiri, M.Uchida and S.Yoda, *J. Jpn. Soc. Microgravity Appl.*, **17**, 64 (2000).
- [41] K. Kinoshita, H. Kato, S. Matsumoto, S. Yoda, J. Yu, M. Natsuisaka, T. Masaki, N. Koshikawa, Y. Nakamura, T. Nakamura, A. Ogiso, S. Amano, K. Goto, Y. Arai, T. Fukazawa, M. Kaneko, T. Itami, *J. Jpn. Soc. Microgravity Appl.*, **17**, 57 (2000).
- [42] J. Yu, M. Natsuisaka, H. Kato, S. Matsumoto, T. Itami K. Kinoshita and S. Yoda, *Rev. Sci. Instrm.*, **71**, 2111 (2000).
- [43] M. Uchida, Y. Watanabe, S. Matsumoto, M. Kaneko, T. Fukazawa, T. Masaki and T. Itami, *J. Non-Crystalline Solids*, 312–314, 203 (2002).
- [44] S. Matsumoto, H. Otsubo, M. Uchida and T. Itami, Proceedings in “The 22nd Japan Symposium on Thermophysical Properties”, Sendai, pp.440 (2001).
- [45] M. Kawaji, *Nuclear Engineering and Design*, **184**, 379 (1998).
- [46] Y. P. Gupta, *Adv. Phys.*, **16**, 333 (1967).

Measurement of diffusion coefficient of Au in liquid Ag due to the shear cell technique

Tadahiko MASAKI^{*1}, Tomoharu FUKAZAWA^{*1}, Yuki WATANABE^{*2},
Minoru KANEKO^{*2}, Shinichi YODA^{*1} and T. ITAMI^{*1*3}

Abstract: Diffusion coefficients of Au in liquid Ag were measured carefully due to the diffusion couple method combined with the shear cell technique at the temperature of 1300 K and 1500 K. The shear cell was so-called modified long capillary crucible and is known to be the best method for the measurement of diffusion coefficient of liquids. The major cause of experimental error was derived from the liquid motion by the connection of liquid sample at the start of diffusion. In the present study, by changing the diffusion time from 300 seconds to seven hours, the time dependence of measured diffusion coefficient was clarified. The effects of the initial disturbance were sufficiently small in the case that the diffusion time was longer than 2 hours, for which the diffusion coefficient became independent on the diffusion time. The diffusion coefficient was compared with the theoretical value which was evaluated from the hard sphere mixture model.

Keywords: Shear Cell, Diffusion, Alloy, Hard sphere model

1. INTRODUCTION

Atomic transport properties are essential and significant to understand disordered condensed matters. Especially, diffusion phenomena play an important role of the reaction and the phase transition process relating to liquid materials. Therefore, the exact value is necessary not only for the understanding of condensed matter physics but also for the improvement of material processing due to numerical simulations, by which the optimization of condition can be obtained, for example, for the process of single crystal growth or the control of microscopic structure of casting. Many efforts have been devoted in order to obtain exactly the diffusion coefficient of liquids [1].

The diffusion couple method is one of the most popular methods for the measurement of diffusion coefficient, in which two pieces of different concentration are contacted as the diffusion sample. Each concentration in both pieces of the diffusion couple develops due to the diffusion, which should obey the Fick's diffusion equation. In the case of liquid sample, the concentration profile due to the diffusion is easily spoiled by the convection in the liquid sample. Therefore, the diffusion sample is contained in a narrow capillary in order to suppress it. This method is called as the long capillary method. Because of its simplicity and easiness for the experiments and for the numerical treatment of data analysis, this method is widely applied to the measurement of diffusion coefficients of liquids. Nevertheless, this long capillary method has some inherent defects for the measurement of diffusion coefficient with high precision. The worst point is excess diffusion; if the experimental temperature is much higher than the melting temperature of sample, the diffusion progresses during the heating and cooling stages. The second one is the bad effect of volume change on melting and solidifying sample. Most of materials change its volume on melting. Therefore, the concentration profile in liquid diffusion sample is spoiled by the fluid motion induced by the volume change. The third one is the segregation on the solidification of diffusion sample. This problem is restricted to alloy samples. Many kinds of alloys show the segregation on solidification. It makes difficult to obtain the concentration profiles of diffusion couple in the liquid state.

The shear cell method was innovated in order to remove these problems. If the two liquid columns can be joined into one liquid diffusion couple and be separated into many pieces at the experimental liquid temperature, it is not necessary to be bothered about these problems. Nachtrieb *et al.* [2] developed for the first time the shear cell for the measurement of self-diffusion coefficient of liquid mercury and

* 1 Japan Aerospace Exploration Agency, 2-1-1 Sengen, Tsukuba, Ibaraki, 305-8505 Japan.

* 2 Advanced Engineering Services Co. Ltd., 1-6-1 Takezono, Tsukuba, Ibaraki, 305-8505 Japan.

* 3 Hokkaido Univ., Sapporo, Hokkaido, 060-0810 Japan

gallium. The shear cell was composed of thin stainless steel disks which can rotate co-axially. Around the center axis the disk possesses a few holes, into which the solid sample was contained. At the experimental temperature, with the rotation of each disk, the liquid sample can be joined into the diffusion couple at the start and separated into many pieces at the end. Barras *et al.* [3] measured the self-diffusion coefficient of liquid thallium. Bruson *et al.* [4, 5] measured the self- and impurity-diffusion of liquid tin in the wide temperature range. Yoda *et al.* [6] measured the self-diffusion coefficient of liquid tin by the refined shear cell method under the microgravity condition. Recently, shear cell method has been applied to molten semiconducting materials and liquid alloys, for example, molten GaSb [7] and aluminum impurity diffusion in liquid gallium and indium [8].

The sample diameters of previous shear cell experiments were typically 1.5 millimeter because of the feasible joining of liquid sample. It was somewhat large to prevent the convection under the normal gravity. Recently, many kinds of novel crucible materials have been developed. The precision of finishing of crucibles can be extremely improved enough to make the refined shear cell whose sample diameter can be less than 1 millimeter. The considerably precise measurement of diffusion coefficient can be performed even on the ground. In this paper, the feature of our shear cell is briefly introduced and the experimental results of the diffusion of Au in liquid Ag are described.

2. MEASUREMENT OF DIFFUSION COEFFICIENT OF AU-AG LIQUID ALLOY DUE TO THE SHEAR CELL METHOD

2.1 Shear cell assembly

In the shear cell, the liquid sample is contained in the long and narrow space in the same manner as the long capillary method. However, this space is composed of the pile of thin disk crucible with small sample holes, which are placed around the center of disk. In the shear cell assembly of the present study, the thickness of disk crucible and the diameter of sample hole were one millimeter respectively. The disk crucible was made of glassy carbon for which the fine machine work can be applied. The end crucibles, spacer and springs were made of sintered carbon. The center rod was made of mullite because of its low thermal conductivity. The diffusion sample, which was cast into the rod shape beforehand, were installed in the shear cell together with small carbon springs and carbon rods as can be seen in figure 1. Each sample of diffusion couple was placed on the separated position before the heating of sample. Liquid diffusion couple was formed and was divided by the rotation of center rod at the experimental temperature. All the shear cell assembly, a ceramic heater and three thermocouples, were covered by the sintered ceramic tube and were fixed on the fitting parts of the observation chamber which was equipped with a two directional X-ray radiography. The inside of observation chamber and that of ceramic tube were evacuated and were filled with high purity argon gas in order to prevent the oxidation of sample and crucible. The feasible joining and dividing of diffusion sample was confirmed by the use of X-ray radiography [9]. Figure 2 shows the X-ray image of diffusion sample in the shear cell. The misalignment of diffusion sample was regarded to be less than 0.1 millimeter which is smaller than the resolution of this X-ray radiography. The temperature of sample was measured by the use of three thermocouples which were installed beside the disk crucible. The temperature of upper part of diffusion couple was 5 K higher than that of lower part due to the optimization of the design of ceramic heater, the amount of thermal insulator and radiation foil around the shear cell assembly.

2.2 Measurement of diffusion coefficient of Au in liquid Ag

For the measurement of diffusion of Au in liquid Ag, the diffusion couple was prepared between pure Ag and $\text{Au}_{0.05}\text{Ag}_{0.95}$. Each material was cased into the graphite crucible and was formed into a narrow rod shape which was one millimeter diameter and 30 millimeter length. Both end faces of diffusion samples were finished with the use of optical fiber polisher. The samples were installed into the shear cell which was described in the sub-section 2.2.

The diffusion coefficients were measured at 1300K, which was 56 K higher than the liquidus temperature, and 1500K. The diffusion time, i.e. from the time of joining into the diffusion couple to that of dividing it, was varied from 300 seconds to 25200 seconds (seven hours) in order to clarify the influence of liquid joining at the start of diffusion. After the diffusion experiments, the shape of each divided sample was changed into thin plate of about 8mm diameter by the repetition of pressing and folding for the measurement of average concentration of overall piece by the X-ray fluorescence analysis.

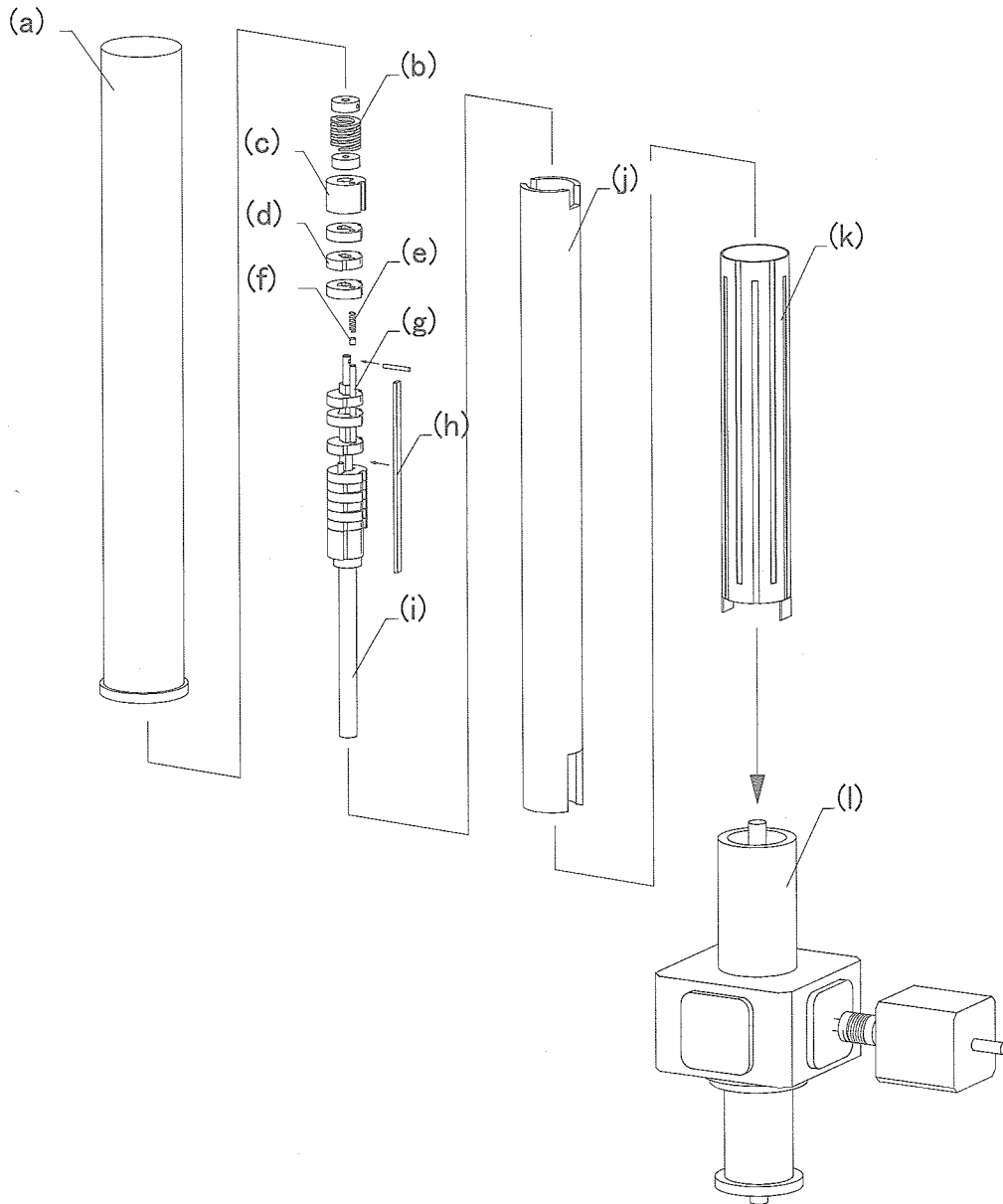


Fig. 1 Shear cell assembly.

(a) ceramic tube; (b) graphite spring; (c) end part; (d) disk crucible; (e) graphite spring; (f) graphite rod; (g) diffusion sample; (h) stop bar; (i) center rod; (j) spacer; (k) ceramic heater; (l) fitting part of observation chamber

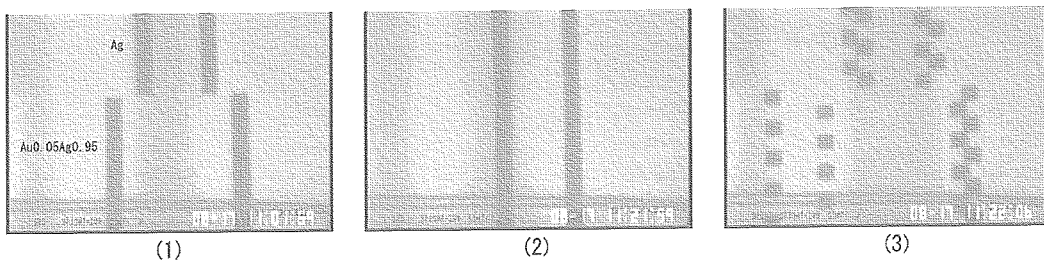


Fig. 2 X-ray image of diffusion sample.

(1): Before joining; (2): Connected; (3): Divided.

3. THE DATA ANALYSIS AND THE EXPERIMENTAL RESULTS

The concentration profile of Au in the sample should obey the error function, which is the analytical solution of the diffusion equation for the present diffusion couple and is given as follows:

$$\frac{2(c(x,t) - c_1)}{c_2 - c_1} = 1 - \text{Erf}(Y). \quad (1)$$

In this equation, c_1 and c_2 are the concentrations of each piece of the diffusion couple at the start of diffusion. The error function, Erf, is defined as follows:

$$\text{Erf}(Y) = \frac{2}{\sqrt{\pi}} \int_0^Y \exp(-y^2) dy \quad (2)$$

The concentration profiles obtained from experiments were in good agreement with equation (2). The typical experimental result is shown in figure 3. The diffusion coefficient of Au in liquid Ag was evaluated by the least square fitting of experimental data to this analytical solution (equation (1)). The diffusion coefficients obtained were strongly depended on the duration of diffusion, as can be seen in figure 4. The observed diffusion coefficient decreased with increasing the duration of diffusion at both 1300 K and 1500 K. From the in situ observation of fluid flow in the model experiment by the use of transparent materials [10], the small amount of liquid is found to be exchanged at the interface of the diffusion couple due to the liquid joining at the start of diffusion. However, the disturbance by the liquid joining becomes negligibly small if the duration of diffusion is sufficiently long, as can be seen figure 3. In the present experiment, the diffusion coefficients were adopted from the diffusion experiments whose durations of diffusion were 21600 second. The diffusion coefficients of Au in liquid Ag are obtained as $2.30 \times 10^{-5} \text{ cm}^2/\text{s}$ at 1300 K and $3.16 \times 10^{-5} \text{ cm}^2/\text{s}$ at 1500 K.

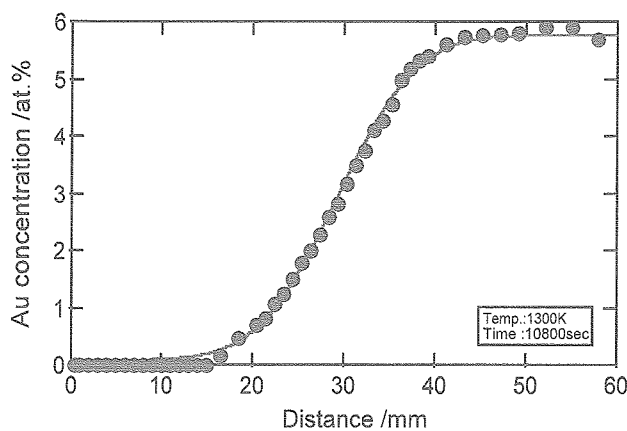


Fig. 3 Diffusion profile of Ag- $\text{Au}_{0.05}\text{Ag}_{0.95}$ diffusion couple.

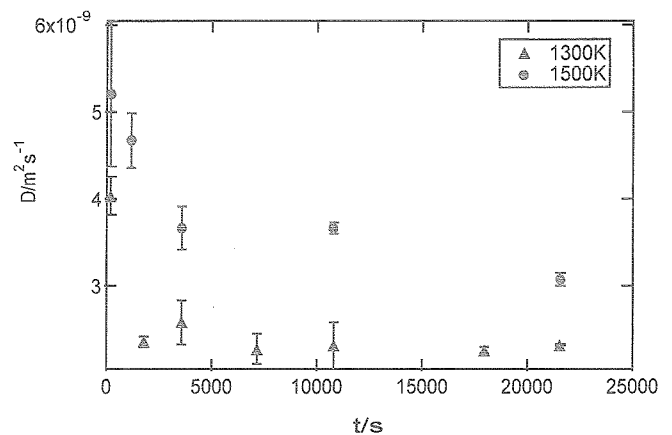


Fig. 4 The diffusion time dependence of diffusion coefficient measured by using the shear cell method.

4. DISCUSSION

The Ag, Au and these alloys are familiar materials for the experiments of liquid metals. However, the self and mutual diffusion coefficient of these systems have not always been measured frequently. In the case of Ag-Au liquid alloys, Gupta [11] published the diffusion coefficients at the temperatures between 1253 K and 1533 K. The diffusion coefficients of present work are slightly lower than Gupta's data. The cause of experimental errors in the previous long capillary method, i.e. the undesirable diffusion on heating and cooling process and the segregation on solidification, may tend to increase the measured diffusion coefficient. The shear cell method adopted here is advantageous for the removal of these errors. In the present experimental configuration, the density of liquid silver in the upper position is lighter than that of Ag-Au alloy in the lower one. Additionally, the temperature of upper part was kept to be about five degrees higher than that of

lower part in order to prevent the convection. The present configuration can suppress the occurrence of the convection in the liquid sample.

The diffusion coefficient of Au in liquid Ag was estimated based on the hard sphere model coupled with the back scattering factor, C_{BS} , given by Protopapas and Parlee [12] and compared with the present experimental results. The diffusion coefficient of a dense binary fluid, D_{HS} , is given as follows;

$$D_{HS} = C_{BS} D_{ENS} . \quad (3)$$

The back scattering factor, C_{BS} , represents the many body effect of dense fluid. In this equation, D_{ENS} is described by the following equation.

$$D_{ENS} = D_{12,g} / g_{12}(\sigma_{12}), \quad (4)$$

where $D_{12,g}$ is the diffusion coefficient of dilute state of mixture whose components are solute 1 and solvent 2. In the case of hard sphere interatomic potential, $D_{12,g}$ is written as follows;

$$D_{12,g} = \frac{3}{8n\sigma_{12}^2} \left\{ \frac{k_B T(m_1 + m_2)}{2\pi m_1 m_2} \right\}, \quad (5)$$

where n is the total number density of mixture; σ_{12} is the mean hard sphere diameter of two components; m_i is the atomic mass of component i , k_B is Boltzman constant; T is the temperature of system. The notation, $g_{12}(\sigma_{12})$, in the equation (4) is the radial distribution function at the contact of different hard spheres. C_{BS} is evaluated from the ratio of the diffusion coefficients obtained from molecular dynamics simulations of hard sphere mixture, D_{HSM} , to the D_{ENS} , as follows;

$$C_{BS} = D_{HSM} / D_{ENS} . \quad (6)$$

Protopapas and Parlee [12] provided the numerical table of C_{BS} of hard sphere mixture, which can be available with the knowledge of the ratio of atomic mass and hard sphere diameter. In this calculation, values of C_{BS} for Ag-Au mixtures are evaluated by the interpolation of the table.

The temperature dependence of hard sphere diameter of pure metal is evaluated from following equation [12].

$$\sigma = 1.228M / d \{1 - 0.112 T / T_m\}^{1/2}, \quad (7)$$

where, M is the mass and d is the mass density at the melting point, T_m . For the calculation of diffusion coefficient of Ag-Au mixtures, it was assumed that the hard sphere diameters of Ag and Au in alloys were equal to those of the pure state respectively. The pure Au becomes solid at 1300K. Therefore, the values of density, d , and hard sphere diameter, σ , are estimated from the extrapolation of the respective temperature dependence at higher temperature than its melting point. The numerical values for this calculation and the diffusion coefficient obtained, D_{HS} , are shown in table 1. The hard sphere model is one of the simplest models for the treatment of liquid properties. Nevertheless, the D_{HS} are in good agreement with present experimental results. Pure Ag and pure Au in liquid state can be regarded as the simple hard sphere fluid based on the liquid structure analysis by Waseda [13]. Ag and Au belong to the same column of periodic table and

Table 1 The comparison of diffusion coefficient of Au in liquid Ag between calculations based on the hard sphere model and experiments.

T (K)	σ_{Ag} (cm)	σ_{Au} (cm)	C_{BS}	D_{HS} (cm ² /s)	D_{exp} (cm ² /s)
1300	2.579×10^{-8}	2.579×10^{-8}	0.6564	2.25×10^{-5}	2.30×10^{-5}
1500	2.556×10^{-8}	2.555×10^{-8}	0.7191	3.07×10^{-5}	3.16×10^{-5}

the charge transfer between Ag and Au in liquids might be small. As the zeroth approximation, the atomic transport properties of Au in liquid Ag can be regarded as the simple hard sphere mixtures. It is possible that this hard sphere model can be improved by taking account of the charge transfer effect and its concentration dependencies on the evaluation of C_{BS} . Such studies must be studied in future.

5. CONCLUSION

The diffusion coefficients of Au liquid in Ag were measured with the use of shear cell method at both 1300K and 1500K. The diffusion coefficient corresponding to the present experimental conditions were calculated by using the hard sphere mixture model. Diffusion coefficients of hard sphere model are in good agreement with the experimental data.

REFERENCE

- [1] M. Shimoji and T. Itami, "Atomic Transport in Liquid Metals", Trans tech publications, Switzerland (1986).
- [2] N.H. Nachtrieb, J. Chem. Phys., 24, 746 (1956).
- [3] R. E. Barras, H. A. Walls and A. L. Hines, Met. Trans., 6B, 347 (1975).
- [4] A. Bruson and M. Gerl, Phys. Rev. B, 21, 5447 (1980).
- [5] A. Bruson and M. Gerl, Phys. Rev. B, 19, 6123 (1979).
- [6] S. Yoda, T. Masaki and H. Oda, NASA-CP-1998-208868, pp.86 (1998).
- [7] G. Muller-Vogt and R. Kossler, J. Cryst. Growth, 186, 511 (1998).
- [8] P. Brauer and G. Muller-Vogt, J. Cryst. Growth, 186, 520 (1998).
- [9] M. Uchida, Y. Watanabe, S. Matsumoto, M. Kaneko, T. Fukazawa, T. Masaki and T. Itami, J. Non-Crystalline Solids, 312–314, 203 (2002).
- [10] S. Matsumoto, H. Otsubo, M. Uchida and T. Itami, Proceedings in "The 22nd Japan Symposium on Thermophysical Properties", Sendai, pp.440 (2001).
- [11] P.Y. Guputa, Adv. Phys., 16, 333 (1967).
- [12] P. Protopapas and N.A.D. Parlee, High Temperature Science, 8, 141 (1976).
- [13] Y. Waseda, "The structure of non-crystalline materials", McGraw-Hill, New York, pp. 52 (1980).

静電浮遊法による高温金属液体の構造解析

正木 匡彦, 石川 毅彦, 依田 真一

Liquid Structure Analysis of High Temperature Molten Metals with the Use of Electrostatic Levitator

By

Tadahiko MASAKI, Takehiko ISHIKAWA, Shinichi YODA

Abstract: The structure of undercooling liquid state is one of the important subjects of materials science. The levitation techniques are powerful tools for the investigation of undercooled liquids. In this research, we developed the electrostatic levitation furnace for the liquid structure analysis due to the neutron and x-ray diffraction methods. The apparatus was tested by using a synchrotron radiation facility, a laboratory X-ray source and a reactor. The structures of several kinds of materials were investigated and the liquid structures can be measured with high precision.

Keywords: Electrostatic levitator, liquid structure, X-ray diffraction, neutron diffraction

概 要

X線・中性子散乱法と静電浮遊炉を組み合わせることにより、超高温や過冷却液体の構造を精密に測定することが可能である。本研究は、シリコンやジルコニウムなど高温金属液体の液体構造を測定するために、構造解析用の静電浮遊炉を新たに開発し、高輝度放射光および中性子線を用いた散乱実験を試みた。実験の結果、これらの液体の静的構造因子（過冷却液体状態を含む）を高精度に測定することができた。

1. 緒 言

過冷却液体状態では、平衡状態の液体には見られないような大規模の濃度揺らぎや二十面体構造のようなクラスター構造が存在しうることが分子動力学計算などにより示唆されている[1]。また、過冷却液体の物性の把握は、ガラスやアモルファス材料など新たな材料の創生において不可欠であり、詳細な研究が待たれている領域である。近年、無容器実験法をもちいた過冷却液体状態の研究が盛んに進められており、静電場法、電磁誘導法やガスジェット法などの手法を用いた過冷却液体の物性・構造研究や凝固過程の研究が進められている[2-6]。その中でも、静電場を用いた液滴浮遊法は、金属・非金属を問わずに浮遊できる点だけでなく、サンプルサイズ（直径1~2 mm）や雰囲気（高真空もしくは高圧）などの実験条件が高温液体の物性計測や構造解析に極めて適した方法である[7]。この静電浮遊法とX線散乱法や中性子散乱法を用いた構造解析を組み合わせることにより、従来測定が極めて困難であった高融点金属液体や過冷却液体状態の構造解析を可能にするだけでなく、吸収や多重散乱の補正を容易にし、測定の精度を著しく向上させることが可能である。

高精度の液体構造の実験値から液体状態の微視的な特徴を知ることができる。特に、過冷却液体に存在すると期待される多面体クラスターや揺らぎ構造は、散乱実験から直接的に得られる静的構造因子や動径分布関数を調べることにより確認することができると考えられる。また、精密に測定された液体構造から、原子間ポテンシャルを決めることが可能である。実験的に決めた原子間ポテンシャルからは、拡散係数や粘性係数などの巨視的な輸送物性だけでなく、液体内の構造の緩和過程の研究や実験では実現不可能な急冷過程をへたガラス状態の可能性などを探索することが可能となる。

JAXAではこれまで、宇宙空間の微小重力環境における浮遊試料の位置制御法として静電浮遊法を開発してきた[8]。良く知られているように、微小重力環境において浮遊させた液滴を用いることにより、極めて高精度の液体物性を測定することが可能である。本研究は、その宇宙実験技術を地上の研究へスピノフしたものであるが、宇宙環境利用と独立したのではなく、宇宙実験による高精度融液体物性データを微視的な立場から理解し補完することを目的としている。

著者らは、過冷却液体状態とくに金属や半導体の過冷却状態の微視的構造を詳細に調べることを目的として、過冷却液体状態を安定して保持できる静電浮遊法とX線散乱または中性子散乱法を組み合わせることにより高精度の液体構造解析装置を製作した。装置の試験を兼ねて、室温の焼結アルミナ球、液体ジルコニウムや液体シリコンなど過冷却液体状態を取りやすい物質の液体構造解析を試み、静的構造因子の取得に成功した。以下に装置および実験の概要を紹介する。

2. 中性子およびX線散乱用の静電浮遊装置

2.1 静電浮遊法の概要

静電場を用いる場合、試料を帯電させることにより金属・非金属を問わず浮遊させることが可能である。本研究では図1に示すように上下に配置した電極の上側に $-10 \sim -30$ kVの電圧を印加し、また正電荷を帯電させた試料を電極間に挿入し、重力と拮抗した上向きの力を発生させた。このような電極と試料の配置では、パッシブな安定点が存在しないことから、試料を電極の中間に保持するためには試料位置の計測と電極間電圧の制御を高速に行う必要がある。本装置は、He-Neレーザー、ポジションディテクタ、高速直流アンプをコンピュータ制御し、約720 Hzの制御サイクルにより安定した浮遊状態を実現した。電極間に高電圧をかけることから、電極と試料は 10^{-4} Pa程度の真空を維持できる高真空チャンバー内に配置した。高真空雰囲気は、熔融させた試料の酸化を防ぐとともに、試料の帯電状態の維持に寄与している。真空中に浮遊させた試料の加熱には、炭酸ガスレーザーを使用した。レーザー光を真空チャンバーの上部に設置したZnSe窓および上側の電極中央の穴を通して試料に照射し、また、試料温度については単色の放射温度計を使用して測定した。真空チャンバーの側面には、X線もしくは中性子線の入射用および散乱強度を検出するための窓を配置した。真空チャンバーは、中性子散乱用とX線散乱用について、ディフラクシオメータの形状や線源の特性を考慮して、それぞれ1台ずつ製作した。検出可能な角度範囲であるが、X線散乱の場合は $2\theta = -10 \sim +80^\circ$ 、中性子散乱の場合は $2\theta = -10 \sim +160^\circ$ である。

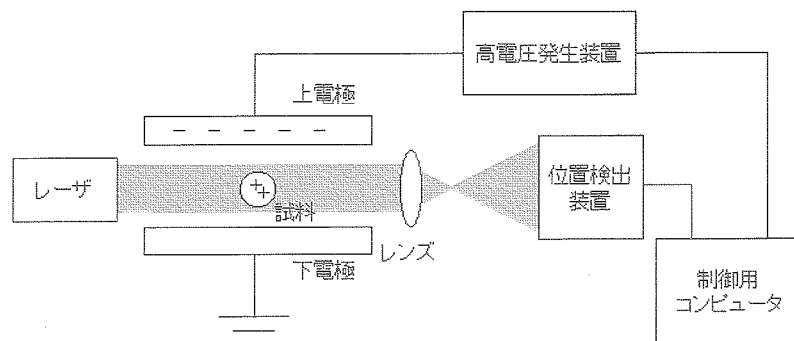


Fig. 1 Schematic figure of position control system of electrostatic levitator.

2.2 中性子散乱実験のための静電浮遊装置

静電浮遊法において、試料電荷の急激な変化は、浮遊制御の不安定化の原因となる。中性子は中性電荷の粒子であり、散乱実験に使用する際に試料との電荷のやり取りがないことから、静電浮遊法に対する適合性が良いと考えられる。

中性子散乱による液体構造測定法に対して静電浮遊炉を適用するために、日本原子力研究所（現日本原子力研究開発機構）との共同研究を行い、東海研究所3号炉の高精度粉末中性子線回折装置（HRPD）を用いた実験を行った[9]。電極を含む真空チャンバーを中性子散乱用のスペクトロメータの幾何構造にあわせて新たに設計・製作した。HRPDは比較的大型の装置であり、試料部周辺の空間が大きく取れることから、静電浮遊炉の真空チャンバーおよび位置検出などの光学系を余裕をもって設置することができる。中性子散乱法の場合、中性子線が照射された物質が放射化されることから、液滴位置検出用の光学系や放射温度計などは、中性子線の光軸から離れた位置に配置し、複数のミラーを持てることで、試料位置の計測と制御を行った。モノクロメータにより単色化された波長 1.823\AA の入射中性子線を使用し、試料により散乱された



Fig. 2 Photograph of electrostatic levitator for neutron diffraction measurement.

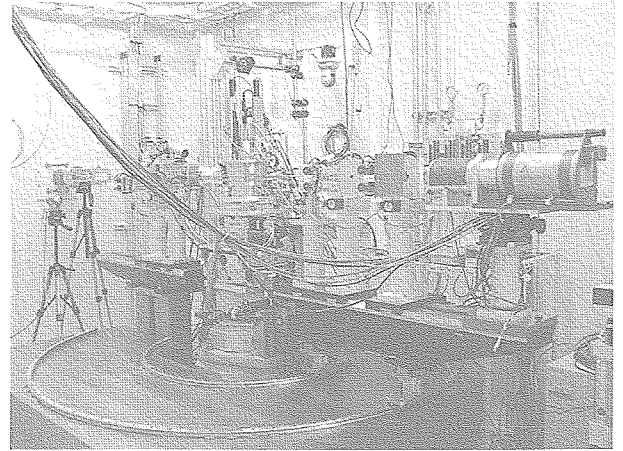


Fig. 3 Photograph of electrostatic furnace for the x-ray diffraction experiment at the SPring-8.

中性子を64個の検出器により同時に検出した。試料の加熱には100 WのCO₂レーザーを使用し、放射温度計を用いてより試料温度を測定した。中性子散乱実験では一般に数ccの容積の試料が用いられるが静電浮遊法では直径2 mm程度の小さな試料しか浮遊させることができない。そのためこの実験では製作した静電浮遊炉の検証のため、散乱強度が明瞭に測定できる焼結アルミナ球と、浮遊溶融が容易なジルコニウムを実験試料として選択した。実験装置の写真を図2に示す。

2.3 X線散乱実験のための静電浮遊装置

X線散乱実験用の真空チャンバーは、実験室のX線回折装置 (Rigaku SWXD) のゴニオメータおよびSPring-8のBL 04 B 2ビームラインに設置されたランダム系ステーションの二軸回折計の両者に設置できるように製作しており、放射光を用いた高精度計測と実験室レベルの試行的実験の両者を効率よく行える設計とした。図3に放射光実験の際の装置の写真を示す。実験では、過冷却液体状態を取りやすいジルコニウムおよびシリコンを対象とし、X線散乱による構造解析を行った。液体のX線構造解析には、一般に試料水平型のゴニオメータを用いて反射法を用いて測定されるが、この実験では、球状の試料からの散乱強度を正確に計測するため、透過法を選択した。透過法の場合、試料によるX線の吸収によって散乱強度が大きく変化することから、試料のX線吸収係数を考慮してジルコニウムには放射光を、シリコンにはMoK α 線を用いることとした。

ジルコニウムの構造解析の場合、113 keVの高エネルギーの単色X線を使用し、二軸回折計、スリット光学系および半導体検出器を用いて透過法による散乱X線の強度の角度分布を測定した。この二軸回折計は、水平方向に検出器を移動するタイプである。今回用いた静電浮遊法は、上下の電極間に試料を保持するため、この二軸回折計を用いることにより真空チャンバーの窓をのぞいて入射・散乱X線の両者をささげざるもの無い理想的な条件の散乱実験が可能である。

シリコンの場合、MoK α に対する吸収係数がそれほど大きくないため、実験室の18 kWのMoK α X線源を用いて透過法による散乱実験を行った。散乱X線強度の検出にはグラファイトのカウンターモノクロメータと比例計数管を使用し、それ以外は、放射光の実験と同様に二軸回折計、スリット光学系を使用した。

3. 実 験

3.1 実験試料の作製

本装置を用いて試料を浮遊させる場合、位置検出の精度や印加可能な最大電圧などから、試料をもっとも安定浮遊保持できる大きさは直径2 mm程度である。本実験では、ジルコニウム、シリコンともに、直径2 mmの球状試料を使用した。試料表面に付着した酸化物などは過冷却液体状態において凝固のきっかけとなるため、表面の清浄性を極力維持できるようにして試料を作成した。直径2 mm程度になるようにあらかじめ秤量した試料を、高純度アルゴンを充填したグローブボックス内の窒化ホウ素基板上に置き、続いて、高出力の半導体レーザー (200 W) を用いて短時間で溶融・凝固させ球状の試料を作成した。シリコンについては99.999%、ジルコニウムについては99.5%の純度の試料を使用した。作成した試料はほぼ完全な球状であり、またジルコニウム・シリコン表面ともに金属光沢を有していた。試料はアルゴン雰囲気の中で試

料瓶に密閉し、さらにアルゴン雰囲気を維持したまた静電浮遊装置のチャンバーに導入した。

3.2 浮遊試料の中性子およびX線散乱計測

静電浮遊法を用いて試料を浮遊溶融させる場合、試料の帯電量を維持することが極めて重要である。しかしながら、室温において浮遊させた試料を加熱した場合、試料表面からの蒸発や残留ガスとの反応により帯電量が減少し、試料の一制御が不安定になる。ジルコニウムおよびシリコンの場合、比較的高融点であることから、浮遊前にあらかじめ試料を加熱し、熱電子放出によって帯電量を増加させながら浮遊させることが可能である。本実験においても、浮遊させる前に試料を1400 K程度に加熱し、安定した浮遊溶融状態を実現した。

試料の加熱・冷却については、炭酸ガスレーザーの出力を制御することにより行った。特に、試料を過冷却液体状態にする際には、試料を融点よりも100 K程度高温に加熱して資料を十分に溶融させ、続いて炭酸ガスレーザーの出力を徐々に下げながら融点以下に冷却した。なお、放射温度計の指示値を常にモニターし、凝固に伴う急激な温度変化やリカレンセンスなどの無いことを確かめることで、過冷却液体状態であることを確認した。

試料の浮遊溶融状態を確認した後に、中性子およびX線源のビームストップを開放し、散乱強度の角度依存性を測定した。中性子散乱については、室温の焼結アルミナ球および融点近傍のジルコニウムの構造を測定し、X線散乱については、試料温度2125 K（融点近傍）、2035 Kおよび1945 Kのジルコニウムおよび試料温度1683 K（融点近傍）のシリコンの液体構造を測定した。

4. 結果と考察

4.1 浮遊アルミナおよび溶融ジルコニウムの中性子散乱実験

室温におけるアルミナの中性子散乱強度の角度依存性を図4示す。固体からのブラッグ散乱は極めて明瞭なピークを示すため、本実験で用いたような小さな試料を用いても明瞭な散乱パターンを得ることができた。融点近傍の液体ジルコニウムについても同様の測定を行った。静電浮遊法により浮遊させたジルコニウム液体の帯電量は、中性子の照射の有無に対して普遍であり、11時間もの長時間の安定した浮遊状態を維持することができた。液体の散乱強度が固体と比較して数百分の一程度と弱いことや試料が小さいことから、実験時間内に十分な統計精度の散乱パターンを得ることができなかったが、液体からの散乱と考えられるブロードな散乱強度を得ることができた。

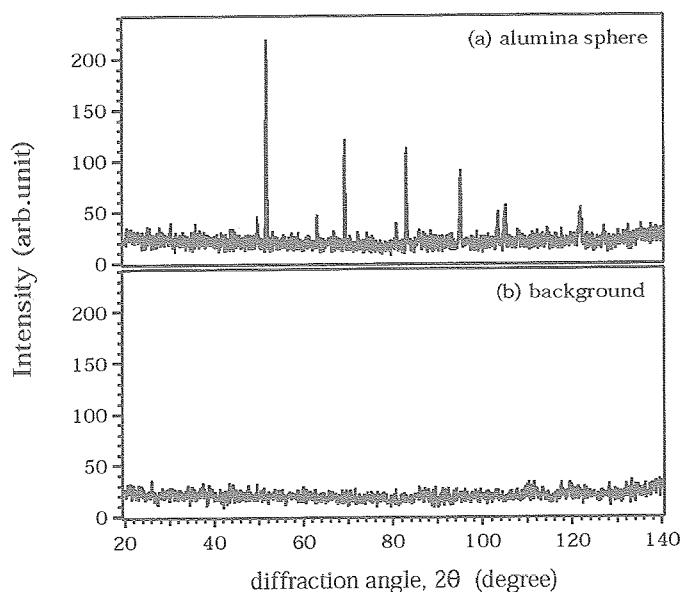


Fig. 4 Diffraction pattern of sintered alumina at room temperature. (a) alumina sphere, (b) diffraction of empty chamber.

4.2 ジルコニウムおよびシリコン液体の X 線散乱実験

透過力の大きな高エネルギー放射光を用いて測定した各温度における液体ジルコニウムの X 線散乱強度の角度依存性および真空チャンバーのみからの散乱（バックグラウンド）を図5に示す。高真空のチャンバーを用いることにより、バックグラウンドの強度をほぼゼロにすることができた。なお、無容器の浮遊状態であることから、試料のみからの散乱を計測できるため、その後のデータ解析を容易かつ高精度に行うことが可能である。また、実験室の X 線源を用いて測定したシリコンの X 線散乱強度の角度依存性を図6に示す。

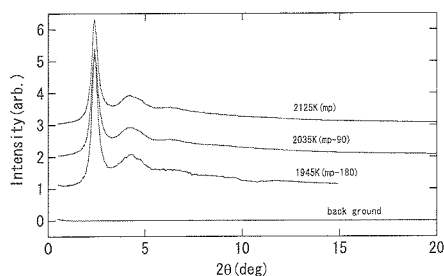


Fig 5 X-ray diffraction patterns of levitated liquid zirconium and empty chamber.

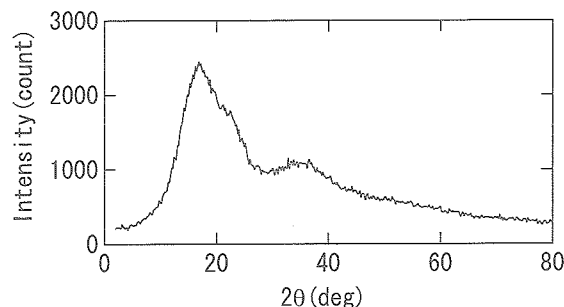


Fig. 6 X-ray diffraction pattern of levitated liquid silicon at melting point.

4.4 吸収と多重散乱の補正

散乱 X 線強度を規格化し、静的構造因子 $S(Q)$ や動径分布関数 $g(r)$ を求める際に、一般的に吸収補正、偏光補正や多重散乱補正などをする必要がある。

$$I^{obs}(Q) = PA [I^{coh}(Q) + I^{inc}(Q) + I^{mul}(Q)]$$

ここで、 I^{obs} は実験で得られた散乱強度、 I^{coh} は弾性散乱強度、 I^{inc} は非弾性散乱強度、 I^{mul} は試料内で2回以上散乱した多重散乱の強度である。 Q は波数であり、散乱角 2θ とは以下の関係がある。

$$Q = 4\pi \sin \theta / \lambda$$

特に、吸収補正と多重散乱補正については、試料形状や吸収係数に大きく依存するため、これまで実験後のデータ解析を困難にしてきた。浮遊液滴を用いた場合、ほぼ真球状の試料形状であるために、これらの補正を比較的容易に、かつ、高精度に行うことが可能である。一般に単結晶の構造解析において球状の試料が用いられることから、X線に完浴させた球状試料の吸収補正に関しては以下の式を用いて計算された数値がデータベース化されて公表されている[10]。

$$A = \frac{1}{V} \int_V \exp(-\mu l) dv$$

ここで l は微小体積 dv で散乱された X 線に関する試料中の光路長であり、 μ は試料の吸収係数である。

しかしながら、本研究で測定したジルコニウムの場合、入射 X 線の幅 (0.7 mm) が試料の直径 (2 mm) よりも小さいため、データベースの値をそのまま用いることができない。また実験室の X 線源を用いたシリコンの場合も吸収がデータベースの範囲を超えるため、公表されているデータと同様の方法を用いて吸収が大きな場合の吸収係数を新たに計算した。得られた吸収補正の角度依存性を図7に示す。

多重散乱については、液体の構造測定に用いられる試料水平式のゴニオメータを使用した反射法による測定の場合について、計算が行われた例はあるが[11]、球状の非晶質試料に関して詳細に計算されたことが無いため、試行的な計算を行い、その大きさを評価した。1回の散乱で検出器に到達する散乱 X 線と、2回の散乱で到達する散乱 X 線の強度をそれぞれ数値的に計算し、その比を観測値に対する多重散乱の割合として評価した。なお、今回の計算では多重散乱において最も寄与の大きな2回の散乱のみを評価した。また数値計算の際に、液体の構造因子 $S(Q)$ が必要となるが、今回は計算を簡単に

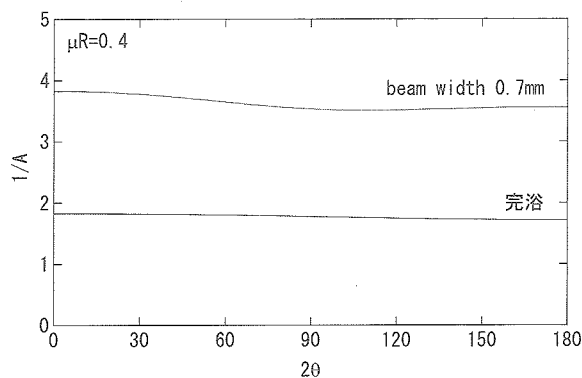


Fig. 7 Correction factor of absorption for X-ray diffraction measurements of liquid zirconium

するため、剛体球液体の構造因子の解析解を使用し、吸収係数および原子散乱因子については放射光を用いたときのジルコニウムの値を使用した。計算の結果、多重散乱は0.2%程度であることが明らかになった。

これらの補正因子を考慮して、X線散乱実験で得られたジルコニウムおよびシリコンの散乱強度からそれぞれの液体の $S(Q)$ を求めた。得られた $S(Q)$ を以下に示す。

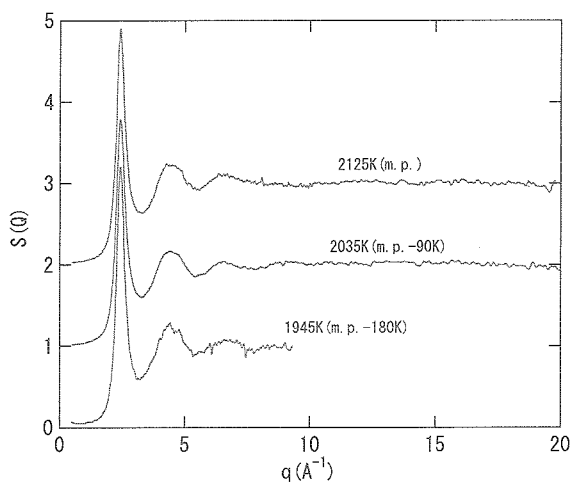


Fig. 8 Static structure factors of liquid zirconium

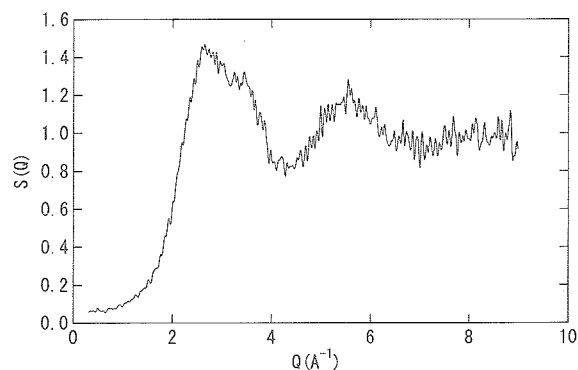


Fig. 9 Static structure factor of liquid silicon at melting point.

4.5 液体構造に基づく有効原子間ポテンシャルの導出

液体論における逆問題の方法を用いることで、静的構造因子から原子間の二体ポテンシャルを求めることができる[12]. Modified Hypernetted Chain (MHNC) 近似から、原子間の有効二体ポテンシャル $u(r)$ を以下のように書くことができる。

$u(r)/k_B T = g_{exp}(r) - 1 - c_{exp}(r) - \ln g_{exp}(r) + B(r)$ ここで、 $g_{exp}(r)$ は実験で求めた動径分布関数、 $c_{exp}(r)$ は直接相関関数であり、静的構造因子から以下の式により求められる。

$$g_{exp}(r) = 1 + \frac{1}{(2\pi)^3 n} \int (S_{exp}(Q) - 1) \exp(-i\mathbf{Q} \cdot \mathbf{r}) d\mathbf{Q} \quad (1)$$

$$c_{exp}(r) = \frac{1}{(2\pi)^3 n} \int \left(1 - \frac{1}{S_{exp}(Q)}\right) \exp(-i\mathbf{Q} \cdot \mathbf{r}) d\mathbf{Q} \quad (2)$$

ここで、 n は数密度である。

逆問題の方法とは、MHNC 近似により求めた原子間ポテンシャルを再帰的に分子動力学計算に用いることで、実験の $S(Q)$ を再現するような $u(r)$ および $B(r)$ を決める方法である。この方法では、 $c(r)$ の式に見られるように $S(Q)$ の逆数の積分を行う必要がため $Q < 1$ の範囲の $S(Q)$ が小さくなる範囲の正確なデータが重要になる。静電浮遊法の場合、容器がないことやバックグラウンドからの散乱がほとんどないため、この範囲の $S(Q)$ を正確に測定することが可能であり、この解析法に適した計測方法と言える。

逆問題の方法を用いる際に、大規模分子動力学計算を行うことで原子間ポテンシャルを高精度に決めることができることが知られている[13]。今回の計算では、約6万個から10万個の原子からなるユニットセルを用いた分子動力学計算を行い、 $u(r)$ を求めた。融点のジルコニウムの $S(Q)$ に対して、得られた原子間ポテンシャルと動径分布関数を図 10 に示す。

有効二体原子間ポテンシャルから、液体の静的および動的物性を計算することが可能である。たとえば、拡散係数 D や粘性係数 (Shear Viscosity) η などの原子輸送物性は、分子動力学計算から以下のように求めることができる。

$$D = \frac{1}{3} \int_0^\infty \langle v(t) \cdot v(0) \rangle dt \quad (3)$$

$$\eta = \frac{1}{k_B T V} \int_0^\infty \langle J_{zx}(t) \cdot J_{zx}(0) \rangle dt \quad (4)$$

$$J_{zx}(t) = \sum_{j=1}^N \frac{1}{m} p_{jz}(t) p_{jx}(t) + \sum_{i=1}^N \sum_{i < j=1}^N z_{ij}(t) f_{ijx}(t) \quad (5)$$

ここで、 v は各粒子の速度、 V は体積、 p_{jz} 、 p_{jx} は粒子 j の z 方向および x 方向の運動量成分、 f_{ijx} は i 番目の粒子から受ける力の x 成分である。現在、ジルコニウムに対するこれらの解析を進めている。液滴振動法による粘性係数の実験値の比較などから、原子間ポテンシャルの妥当性が評価できると考えられる。なお、現時点では解析が十分ではないため、詳細な結果については別の機会に紹介したい。

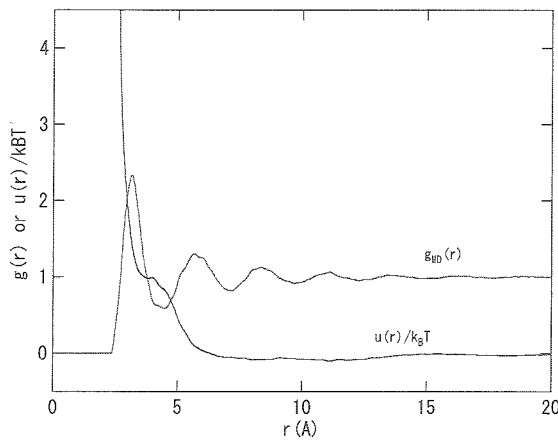


Fig. 10 Effective pair potential and radial distribution function of liquid zirconium at melting temperature

5. 結 言

静電浮遊法およびX線構造解析法を用いて、融点近傍および過冷却液体状態のジルコニウムとシリコンの液体構造の解析を試みた。浮遊液滴試料を用いることにより、試料のみのからくる散乱X線強度を計測できることが実験的に示された。この手法を用いることで、超高温融体や極めて深い過冷却液体状態の構造の研究や輸送物性の理論計算を進めることが可能であるとともに、過冷却液体状態に発現する特異的な物性の予測できる可能性を有している。本研究が、将来の微小重力環境を利用した過冷却液体の熱物性研究のきっかけとなることを期待する。

参 考 文 献

- [1] N.Jaske O. Le Bacq and A. Pasturel., *Phys. Rev. B*, **70** (2004), 174203.
- [2] T.Ishikawa, P.-F Paradis; T.Itami and S. Yoda, *Meas. Sci. Technol.* **16** (2005), 443–451.
- [3] K. Higuchi et al. *Meas. Sci. Technol.* **16** (2005), 381–385.
- [4] S. Krishnan and D. Price, *J. Phys: Cond. Matter*, **12** (2000), R 145–R 176.
- [5] K. Kelton, G.W. Lee, A. K. Gangopadhyay, R. W. Hyers, T. J. Rathz, J. R. Rogers, M. B. Robinson and D. S. Robinson, *Phys. Rev. Lett.*, **90** (2003), 195504.
- [6] D. Holland-Moritz, D. M. Herlach and K. Urban, *Phys. Rev. Lett.*, **71** (1993), 1196.
- [7] W.-K. Rhim, S. K. Chang, D. Barber, K. F. Man and G. Gutt, *Rev. Sci. Instrum.*, **64** (1993), 2961.
- [8] T. Ishikawa, P.-F. Paradis, and S. Yoda, *J. Japan Microgravity Appl.*, **18** (2001), 106.
- [9] H. Aoki, P.-F. Paradis, T. Ishikawa, T. Aoyama, T. Masaki, S. Yoda, Y. Ishii, and T. Itami, *Ref. Sci. Instrum.*, **74** (2003), 1147.
- [10] A.J.C. Wilson and E. Price (ed.), “International Table for Crystallography”, vol.C (1999), 594–596.
- [11] B.E. Warren and R.L. Mozzi, *Acta. Cryst.*, **21** (1966) 459–461.
- [12] L. Reatto, D. Levesque and J. J. Weis, *Phys. Rev. A*, **33** (1986), 3451.
- [13] S. Munejiri, F. Shimojo, K. Hoshino and M. Watabe, *J. Phys. Soc. Japan*, **64** (1995), 344.

JAXA Research and Development Report JAXA-RR-05-034E

Date of Issue: March 8, 2006

Edited and Published by: Japan Aerospace Exploration Agency
7-44-1 Jindaiji-higashimachi, Chofu-shi, Tokyo 182-8522, Japan
URL: <http://www.jaxa.jp/>

Printed by: TOKYO PRESS Co., Ltd.

Inquires about copyright and reproduction should be addressed to the Aerospace Information Archive Center, Information Systems Department, JAXA.

2-1-1 Sengen, Tsukuba-shi, Ibaraki 305-8505, Japan
phone: +81-29-868-5000 fax: +81-29-868-2956

Copyright ©2006 by JAXA.

All rights reserved. No part of this publication may be reproduced, stored in retrieval system or transmitted, in any form or by any means, electronic, mechanical, photocopying, recording, or otherwise, without permission in writing from the publisher.

